QED $O(\alpha^3)$ RADIATIVE CORRECTIONS TO THE REACTION $e^+e^- \to \tau^+\tau^-$ INCLUDING SPIN AND MASS EFFECTS

BY S. JADACH AND Z. WĄS

Institute of Physics, Jagellonian University, Cracow*

(Received April 5, 1984)

We calculate spin amplitudes in QED to order α^3 for the process $e^+e^- \to \tau^+\tau^-(\gamma)$, taking into account effects due to the finite τ mass. The Monte Carlo method is used to simulate directly the production and decay of the τ leptons. Effects of radiative corrections on the momenta of the decay products are investigated. A quantitative discussion of the correlations induced by the spin in the double τ decay is presented. Z_0 exchange is included in the low energy approximation.

PACS numbers: 12.20.Ds

1. Introduction

In this paper we examine the QED to order α^3 radiative and electroweak corrections to the process $e^+e^- \to \tau^+\tau^-$ in the energy range from the production threshold to the highest PETRA/PEP energies. Since the τ is observed only through its decay products, and the parity violating decay of the τ is sensitive to its polarization, it is essential to consider spin effects in this process. Although collisions of unpolarized beams in the lowest order QED yield τ pairs with each τ unpolarized, we still have correlations between the two decays because of spin effects. Spin effects and radiative corrections depend on the τ mass. Thus, in order to realistically describe $e^+e^- \to \tau^+\tau^-$, we have to include radiative corrections, spin and mass effects at the same time.

The first step towards this complete description of the process was presented in Ref. [1] where results from Ref. [2] were re-examined and simplified so that they could serve to construct a Monte-Carlo (M.C.) program which includes mass effects but still no spin effects.

There is, however an important technical difference between the present work and other papers on radiative QED corrections like [1], [2] and [3]. In this paper we calculate

* Address: Instytut Fizyki, Uniwersytet Jagielloński, Reymonta 4, 30-059 Kraków, Poland.

QED corrections to spin amplitudes rather than to differential cross sections. It is somewhat similar to Ref. [4] but we do include masses and we do control the phases of the amplitudes.

There are some reasons to use spin amplitudes. For example we have fewer terms on the level of amplitudes coming from different graphs. Squaring the sum of amplitudes introduces many interference terms. Furthermore for hard bremsstrahlung amplitudes there are useful gauge cancellations which simplify the amplitudes before we calculate the differential cross section with them.

In the numerical results presented in this paper we assumed that beam particles are not polarized, but since we work with spin amplitudes it will be rather easy to include beam polarization in the future, if necessary. That would be more difficult to do if we used the standard $(1+\gamma_5 \not{s})(\not{p}+m)$ projection operators. In the numerical applications we use the density matrix formalism, i.e. the standard polarization vectors. Although we could multiply directly the spin amplitudes for production and decay, we tried to avoid that in order to keep separate both production and decay in the M. C. simulation as much as possible. The reason is that some coupling contants for the τ decay still have to be determined. We also want to keep open the possibility to apply our results to other heavy leptons and quarks. Usually these particles will decay in different ways.

At PETRA/PEP energies the exchange of the weak Z_0 boson may produce a charge asymmetry and a τ polarisation. Thus we include in our calculations Z_0 exchange in a form sufficient for that energy range, i.e. in the lowest order. We remark also that for the future inclusion of Z_0 in the full resonance form there are two possible steps. One may include Z_0 using $m_\tau \ll M_Z$ as an approximation. That can be done relatively easy because some results from Refs [5] and [6] still may be used. It will be more difficult to extend our calculations to fermions with mass comparable with the Z_0 mass like the still hypothetical t-quark or any new heavy lepton.

The layout of the paper is as follows. In Section 2 we introduce the notation and, using the lowest order case as an example, we discuss the connection between spin amplitudes and the density matrix. Also a qualitative discussion of spin correlations is given. Section 3 contains the formulae for radiative corrections of the virtual and soft bremsstrahlung type. In Section 4 we examine hard bremsstrahlung and in Section 5 we present results of the numerical M. C. calculations including a quantitative discussion of the decay correlations induced by spin effects. In Section 6 we summarize our results.

2. Lowest order spin amplitudes and spin effects

In this Section we shall introduce the notation and discuss some spin effects in lowest order. In particular we shall discuss the transition from the spin amplitudes to the density matrix. A brief discussion of the spin correlations is also given at the end of this Section. Some of the results presented in this Section may be found in Ref. [7] but we include them for the sake of completeness and in order to introduce some notations, concepts and methods on the simple example of the lowest order calculations.

The lowest order one photon exchange amplitude for the process $e^+(p_1)+e^-(p_2) \to \tau^+(q_1)+\tau^-(q_2)$ reads

$$M^0_{\lambda_1\lambda_2\alpha_1\alpha_2} = \frac{ie^2QQ'}{(p_1+p_2)^2} V^\mu_{\lambda_1\lambda_2}\tilde{V}_{\alpha_1\alpha_2\mu}, \tag{2.1}$$

where

$$V^\mu_{\lambda_1\lambda_2} = \bar{v}(p_1\lambda_1)\gamma^\mu u(p_2\lambda_2),$$

$$\tilde{V}^\mu_{\alpha_1\alpha_2} = \bar{u}(q_2\alpha_2)\gamma^\mu v(q_1\alpha_1).$$

Here Q and Q' denote the positron and τ^+ charges. The quantities λ_1 and λ_2 are spin projections for e^+ and e^- onto the positron c.m.s. momentum $\vec{p}_1$, i.e. λ_1 and $-\lambda_2$ are the helicities of e^+ and e^- (up to phase conventions). Similarly, α_1 and $-\alpha_2$ are the helicities of τ^+ and τ^-. The vector vertices V and $\tilde{V}$ can be found in Appendix A together with other vertices like scalar, pseudoscalar, axial-vector and tensor which are used in Section 3. Neglecting the electron mass we may write

$$V^\mu_{\lambda_1\lambda_2} = 2(|\lambda_+|\tau^\mu + i\lambda_+\sigma^\mu),$$

$$\tilde{V}^\mu_{\alpha_1\alpha_2} = 2(|\alpha_+|\tau^\mu - i\alpha_+\sigma'^\mu - M\alpha_-\varrho'^\mu), \tag{2.2}$$

where $\tau = (0, 1, 0, 0)$, $\sigma = (0, 0, 1, 0)$, $\varrho' = (0, 0, -\sin\theta, \cos\theta)$ and $\sigma' = (0, 0, \cos\theta, \sin\theta)$ in the c.m. system, defined uniquely by $p_1 = (1, 0, 0, 1)$, $p_2 = (1, 0, 0, -1)$ and $q_1 = (1, 0, -\beta'\sin\theta, \beta'\cos\theta)$. As in Ref. [1] we use $E = ((p_1+p_2)^2)^{1/2}/2$ as an energy unit and $\beta' = (1-M^2)^{1/2}$ where M is the τ mass in units of E, $M = m_\tau/E$. We shall put $\beta = (1-m^2)^{1/2} \to 1$ and $m = m_e/E \to 0$ wherever it is possible. We also introduce the shorthand notation $\alpha_\pm = \alpha_1 \pm \alpha_2$ and $\lambda_\pm = \lambda_1 \pm \lambda_2$ to make the formulae more compact. The resulting spin amplitudes for the lowest order read

$$M^0_{\lambda_1\lambda_2\alpha_1\alpha_2} = iU(-|\lambda_+\alpha_+| - \lambda_+\alpha_+c - iM\lambda_+\alpha_-s), \tag{2.3}$$

where $c = \cos\theta$ and $s = \sin\theta$, $U = e^2QQ'$.

On the other hand we can deal with spin 1/2 fermions using standard techniques, i.e. projection operators

$$\Lambda_\pm(p, w) = (1+\gamma_5 \not{w})(\not{p} \pm M). \tag{2.4}$$

We shall show in our simple example how one can relate spin amplitudes in the form (2.3) to the results obtained using the operators $\Lambda_\pm$. With the standard techniques for unpolarized beam particles, but keeping the final state polarisation vectors w_1 and w_2, we obtain [7]

$$\tfrac{1}{4}\sum_{\lambda_i} M^0(M^0)^* = \tfrac{1}{2}U^2\{(p_1\cdot q_1)^2 + (p_1\cdot q_2)^2 + (p_1\cdot p_2)M^2$$

$$2(w_1\cdot w_2)[(p_1\cdot q_1)(p_1\cdot q_2) - \tfrac{1}{2}(p_1\cdot p_2)M^2] - 2(w_1\cdot p_1)(w_2\cdot p_2)(p_1\cdot q_2)$$

$$-2(w_1\cdot p_2)(w_2\cdot p_1)(p_1\cdot q_1)\} = U^2(R^0_{00} + \sum_{i,k=1}^{3} R^0_{ik}w^i_1 w^k_2). \tag{2.5}$$

In the last formula the index $i = 1, 2, 3$ numbers the three components of $\vec{w}_1$ in the rest frame of the τ^+ lepton and the $k = 1, 2, 3$ numbers the axes in the rest system of the τ^- lepton. In both rest frames the third axis is the spin quantisation axis as in the definition of α_1 and α_2 and the first axis is defined to be perpendicular to the reaction plane i.e. along τ-vector. In (2.5) the absence of terms linear in w_k like $\sum_k R^0_{0k} w_2^k$ and $\sum_k R^0_{i0} w_1^i$ means that each $\tau^\pm$ separately is not polarized in the lowest order. There are, however, correlations between w_1 and w_2 which are controlled by the matrix R^0_{ik}. We extend the matrix R^0_{ik} to R^0_{ab} with $a, b = 0, 1, 2, 3$ obtaining

$$R^0_{ab} = \begin{bmatrix} 1+c^2+M^2s^2, & 0, & 0, & 0 \\ 0, & -(1-M^2)s^2, & 0, & 0 \\ 0, & 0, & (1+M^2)s^2, & 2Mcs \\ 0, & 0, & 2Mcs, & 1+c^2-M^2s^2 \end{bmatrix}. \tag{2.6}$$

In order to calculate the matrix R^0_{ab} as given by equation (2.6) directly from our spin amplitudes defined in Eq. (2.3), we have to translate the bispinor indices in the joint density matrix given by

$$\varrho^0_{\alpha_1\bar{\alpha}_1\alpha_2\bar{\alpha}_2} = \tfrac{1}{4} \sum_{\lambda_1\lambda_2} M^0_{\lambda_1\lambda_2\alpha_1\alpha_2} (M^0_{\lambda_1\lambda_2\bar{\alpha}_1\bar{\alpha}_2})^*$$

$$= \tfrac{1}{2} U^2 \left[|\alpha_+\bar{\alpha}_+| + \alpha_+\bar{\alpha}_+ c^2 + M^2 s^2 \alpha_-\bar{\alpha}_- - \frac{i}{2}(\alpha_+\bar{\alpha}_- - \alpha_-\bar{\alpha}_+) 2Mcs \right] \tag{2.7}$$

into vector indices a and b, see (2.6). The answer may be read off from Eq. (2.4) by substituting in the operator $\Lambda_\pm(p, w)$ as polarisation vectors the three space-like vectors $\hat{e}_1 = (0, 1, 0, 0)$, $\hat{e}_2 = (0, 0, 1, 0)$ and $\hat{e}_3 = (0, 0, 0, 1)$ and comparing the results with the bispinor quantities $u(p, \alpha)\bar{u}(p, \bar{\alpha})$ in the τ rest frame, $p = (M, 0, 0, 0)$, α being the spin projection onto $\vec{e}_3$. The result is

$$\begin{aligned} \Lambda_+(p, \hat{e}_1) - \Lambda_+(p, 0) &= \tilde{\Lambda}_+(p, e_1) = u(p, +)\bar{u}(p, -) + u(p, -)\bar{u}(p, +), \\ \Lambda_+(p, \hat{e}_2) - \Lambda_+(p, 0) &= \tilde{\Lambda}_+(p, e_2) = iu(p, -)\bar{u}(p, +) - iu(p, +)\bar{u}(p, -), \\ \Lambda_+(p, \hat{e}_3) - \Lambda_+(p, 0) &= \tilde{\Lambda}_+(p, e_3) = u(p, +)\bar{u}(p, +) - u(p, -)\bar{u}(p, -), \end{aligned} \tag{2.8}$$

and in addition

$$\Lambda_+(p, 0) = \tilde{\Lambda}_+(p, 0) = u(p, +)\bar{u}(p, +) + u(p, -)\bar{u}(p, -).$$

Similarly Λ_- can be expressed in terms of $v(p, \alpha)\bar{v}(p, \bar{\alpha})$, see Appendix A. In practice, instead of employing directly the relations (2.8) to translate the sixteen elements of the joint density matrix in spinor notation into the sixteen elements of R_{ab} we rather introduce some sort of vocabulary which maps factors like $|\alpha_+\bar{\alpha}_+|$, $\alpha_+\bar{\alpha}_+$ etc. into elements of R_{ab}. For instance $\varrho_{\alpha_1\bar{\alpha}_1\alpha_2\bar{\alpha}_2} = \frac{1}{2}U^2|\alpha_+\alpha_+|$ yields the non-zero elements $R_{00} = 1, R_{11} = -1, R_{22} = 1$, $R_{33} = 1$; all other elements vanish. The complete set of the relations of this type is also

given in Appendix A. Using these relations we obtain from (2.7) the same result for R_{ab} as in Eq. (2.6). In the M.C. calculations the transition from the spin amplitudes to the joint density matrix R_{ab} will usually be done numerically. Thus we deal with spin amplitudes in the analytical calculations and use the density matrix formalism for the M. C. simulation.

Having calculated the matrix R^0_{ab} let us now discuss briefly and qualitatively the spin correlations in the lowest order in two limits. In the energy range far above the threshold ($M \to 0$ limit) the matrix R^0_{ab} simplifies to the following form

$$R^0_{ab} = \begin{bmatrix} 1+c^2, & 0, & 0, & 0 \\ 0, & -s^2, & 0, & 0 \\ 0, & 0, & s^2, & 0 \\ 0, & 0, & 0, & 1+c^2 \end{bmatrix}. \tag{2.9}$$

The positive spin correlation resulting from $R^0_{33} = 1+c^2$ is called here the longitudinal spin correlation. As we shall see in Section 5, it causes positive correlations between c.m. energies of the decay products. Longitudinal spin correlation results from helicity conservation. Note that because the electron is nearly massless, the intermediate photon has its spin aligned with the beam axis. That explains why we have the positive spin correlation for the second axis, $R^0_{22} = s^2$, which is perpendicular to the τ momentum but coplanar with the beam. Finally the correlation $R^0_{11} = -s^2$ simply reflects the angular momentum conservation. The two latter correlations we call transverse spin correlations. They induce specific correlations in the transverse momenta of the decay products with respect to the τ^+ momentum which will be discussed in Section 5.

The second energy regime is the energy near threshold, ($M \to 1$ limit). There we have $R^0_{00} = 2$, $R^0_{22} = 2s^2$, $R^0_{33} = 2c^2$, $R^0_{23} = R^0_{32} = 2cs$, the other elements vanish. As we see, the spins of the τ's try to align both in the same direction along the beam axis. Summarizing, the pattern of the correlations is not simple and varies with energy. There is no doubt that a M.C. simulation is the most efficient way to examine these correlations quantitatively and to include them in the data analysis.

3. Virtual and soft photon corrections

In this Section we discuss the $O(\alpha^3)$ corrections to the spin amplitudes in the case when no hard photon is emitted. First we examine the corrections to the spin amplitudes which are proportional to the lowest order spin amplitudes. They include the vacuum polarization, the electric part F_1 of the initial and final state vertex correction and the soft photon bremsstrahlung. Then we come to the box diagram contributions and to the contribution from the magnetic part F_2 of the final state vertex correction. Lowest order amplitudes do not factorize for the second group of corrections and this is why we discuss them separately.

The lowest order spin amplitudes together with the electric part F_1 of the initial and final state vertex correction and vacuum polarization Π may be written as follows

$$M^{\mathrm{VP}}_{\lambda_i\alpha_i} = M^0_{\lambda_i\alpha_i}(1+F_1(m^2)+\tilde{F}_1(M^2)-\Pi), \tag{3.1}$$

where $M^0_{\lambda_i\alpha_i}$ is defined in Eq. (2.3). The amplitude for the soft photon emission factorizes into M^0 and the typical infrared-divergent factor

$$M^{\pm} \sim eM^0 \left\{ Q \left[-\left(\frac{p_1}{k \cdot p_1} = \frac{p_2}{k \cdot p_2} \right)^2 \right]^{1/2} \right.$$

$$\left. + Q' e^{\pm i\varphi} \left[-\left(\frac{q_1}{k \cdot q_1} - \frac{q_2}{k \cdot q_2} \right)^2 \right]^{1/2} \right\}, \tag{3.2}$$

where $k = (E_\gamma, \vec{k})$ is the momentum of photon and φ is the angle between the planes spanned by $(\vec{k}, \vec{p}_1)$ and $(\vec{k}, \vec{q}_1)$ as in Ref. [4]. The $\pm$ sign denotes the two possible circular polarizations of the emitted soft photon. The formula (3.2) can be obtained easily as an $E_\gamma \to 0$ limit of the hard bremsstrahlung amplitudes calculated in the next Section. In order to obtain the differential cross section or the density matrix elements we take the square[1] of (3.1) and of (3.2), then integrate over the photon momentum with the usual cut-off $E_\gamma < k_0$ and add them, summing over the photon polarizations $\pm$ and fermion spins λ_i, α_i if necessary. Infrared divergences of the C-even part of the soft bremsstrahlung cancel with the infrared divergences of vertex corrections F_1 and $\tilde{F}_1$ for density matrix elements in the same way as for spin-summed unpolarized cross sections. The reason is that all spin dependence is isolated in the factor $M^0_{\lambda_i\alpha_i}$. As a result the corrected correlation matrix R_{ab} takes the simple factorized form

$$R^s_{ab} = R^0_{ab} \left\{ 1 + \delta^{SX}(m^2, k_0) + \delta^{SX}(M^2, k_0) - 2 \operatorname{Re} \Pi + \frac{\alpha}{\pi} QQ' \right.$$

$$\left. \times \left[4 \ln k_0 \ln \frac{1-\beta' c}{1+\beta' c} + D(\beta' c) - D(-\beta' c) \right] \right\}. \tag{3.3}$$

The functions $\delta^{SX}(m, k_0)$ and $D(\beta' c)$ are defined in Ref. [1]. In Eq. (3.3) we included also the infrared singular part of the box diagrams which cancel the infrared divergence from the C-odd part of the soft bremsstrahlung. We remark that formula (3.3) generalizes trivially to the case of polarized beams. Obviously R_{00} agrees also with the spin-summed differential cross section obtained in Ref. [1]. Formula (3.3) was also verified independently using the operators (2.4) instead of spin amplitudes.

The useful property of factorization in Eq. (3.2) and (3.3) does not hold any more for box diagrams. Instead of presenting the complete but lengthy derivation of the spin amplitudes for the box diagrams we shall give in this Section a brief summary of the results for box amplitudes and we refer the reader to Appendix B for more details.

The final result for the spin amplitudes of an uncrossed box diagram reads

$$M^a_{\lambda_i\alpha_i} = \frac{\alpha}{2\pi} QQ' \{ (-iM^0_{\lambda_i\alpha_i}) X_0 - U(|\lambda_+\alpha_+| X_1 + \lambda_+\alpha_+ X_2 + i\lambda_+\alpha_- M X_3) \}. \tag{3.4}$$

[1] Only the lowest order and $O(\alpha^3)$ terms are kept.

All functions X_i can be expressed in terms of four basic functions $\tilde{A}$, $\tilde{B}$, F'_A and F'_Q which are defined in Appendix B. The decomposition is

$$X_0 = -\pi\tilde{A} + i\tilde{A}\ln\frac{\lambda^2}{4}$$

and for $k = 1, 2, 3$

$$X_k = \sum_{j=1}^{6} c_{kj}A_j = c_{k1}i\tilde{A} + c_{k2}(-\pi\tilde{A} + i\tilde{B}) + c_{k3}F'_A$$

$$+ c_{k4}F'_Q + c_{k5}\left(2\pi + i\ln\frac{4}{m^2} + i\ln\frac{4}{M^2}\right) + c_{k6}i\left(\ln\frac{4}{m^2} - \ln\frac{4}{M^2}\right). \tag{3.5}$$

The (small) photon mass is denoted by λ and the coefficients c_{kj} depend on $c = \cos\theta$, $s = \sin\theta$, $\omega = 2 - 2\beta' c - M^2$ and are listed in Table I.

TABLE I

The coefficients c_{ik} in the formula (3.5) for function X_i in the box amplitude

k \ j	1	2	3	4	5	6
1	$\frac{\beta'(\beta' - c)}{\omega}$	$\frac{\omega}{2\beta'^2 s^2} - 1$	$\frac{\omega}{2\beta'^2 s^2}$	$1 - \frac{\omega c}{2s^2\beta'}$	$-\frac{1}{2}$	$\frac{1-\beta'^2}{2\omega}$
2	$\frac{\beta' - c}{\omega}$	$-\frac{c\omega}{2\beta'^2 s^2}$	$c\left(1 - \frac{\omega}{2\beta'^2 s^2}\right)$	$\frac{\omega}{2s^2\beta'} + c - \beta'$	$-\frac{1}{2\beta'}$	$\frac{1-\beta'^2}{2\beta'\omega}$
3	$-\frac{s}{\omega}$	$-\frac{\omega}{2\beta' s}$	$s\left(1 - \frac{\omega}{2\beta'^2 s^2}\right)$	$\frac{c\omega}{2\beta' s}$	0	$\frac{s}{\omega}$

The contribution from the second, crossed box diagram may be obtained by the replacement $X_i(c, s) \to \pm X_i(-c, -s)$ where the minus sign should be taken only for $i = 1$.

To obtain the $O(\alpha^3)$ contribution to the cross section and to the density matrix we take the interference of the box amplitude with the lowest order amplitudes. Averaging over the electron spins we obtain

$$\varrho^{\mathrm{a}}_{\alpha_i\bar{\alpha}_i} = \tfrac{1}{4}\sum_{\lambda_i}(M^{\mathrm{a}}_{\lambda_i\alpha_i}(M^0_{\lambda_i\bar{\alpha}_i})^* + M^0_{\lambda_i\alpha_i}(M^{\mathrm{a}}_{\lambda_i\bar{\alpha}_i})^*)$$

$$= QQ'\frac{\alpha}{\pi}\varrho^0_{\alpha_1\bar{\alpha}_1\alpha_2\bar{\alpha}_2}\,\mathrm{Im}\,X_0 + QQ'\frac{\alpha}{2\pi}U^2\Big[|\alpha_+\bar{\alpha}_+|\,\mathrm{Im}\,X_1$$

$$+ \alpha_+\bar{\alpha}_+ c\,\mathrm{Im}\,X_2 + \alpha_-\bar{\alpha}_- M_s^2\,\mathrm{Im}\,X_3 - \frac{i}{2}(\alpha_+\bar{\alpha}_- - \alpha_-\bar{\alpha}_+)M$$

$$\mathrm{Im}\,(sX_2 + cX_3) + \tfrac{1}{2}(\alpha_+\bar{\alpha}_- + \alpha_-\bar{\alpha}_+)M\,\mathrm{Re}\,(-sX_2 + cX_3)\Big]. \tag{3.6}$$

Using relations from Appendix A, we can write down explicit expressions for the box contribution to the correlation matrix. The non-zero elements are as follows

$$R^{a}_{00} = \frac{\alpha}{\pi} QQ' \operatorname{Im}(X_1 + cX_2 + M^2 sX_3),$$

$$R^{a}_{11} = \frac{\alpha}{\pi} QQ' \operatorname{Im}(-X_1 + cX_2 + M^2 sX_3),$$

$$R^{a}_{22} = \frac{\alpha}{\pi} QQ' \operatorname{Im}(X_1 - cX_2 + M^2 sX_3),$$

$$R^{a}_{33} = \frac{\alpha}{\pi} QQ' \operatorname{Im}(X_1 + cX_2 - M^2 sX_3),$$

$$R^{a}_{23} = R^{a}_{32} = \frac{\alpha}{\pi} QQ' \operatorname{Im}(MsX_2 + McX_3),$$

$$R^{a}_{01} = R^{a}_{10} = \frac{\alpha}{\pi} QQ' \operatorname{Re}(-MsX_2 + McX_3). \tag{3.7}$$

We have neglected the infrared singular part $\frac{\alpha}{\pi} QQ' R^{0}_{ab} \tilde{A} \ln \frac{\lambda^2}{4}$ which has been already absorbed into the previously discussed group of corrections given in Eq. (3.3). The second, crossed box contribution is

$$R^{b}_{ab}(c, s) = -R^{a}_{ab}(-c, -s). \tag{3.8}$$

We have checked that R^{a}_{00} agrees with the result obtained in Ref. [1]. We have also verified that one obtains the same result for R^{a}_{ab} using spin projection operators (2.4) instead of spin amplitudes (3.4).

The contribution from the magnetic part of the final vertex correction is not proportional to $M^{0}_{\alpha_i \lambda_i}$, like in the case of the box diagram contribution. This may be seen from its spin amplitudes which are given by

$$i \frac{1}{M} \tilde{F}_2(M) (-|\lambda_+ \alpha_+| M - i\lambda_+ \alpha_- s - \lambda_+ \alpha_+ Mc). \tag{3.9}$$

The contribution to the R-matrix is obtained by taking the interference of (3.9) with the lowest order amplitudes. The following non-zero elements are obtained:

$$R^{m}_{00} = 4 \operatorname{Re} \tilde{F}_2,$$

$$R^{m}_{01} = R^{m}_{10} = -2(1 - M^2) cs \operatorname{Im} \tilde{F}_2 / M,$$

$$R^{m}_{22} = 4s^2 \operatorname{Re} \tilde{F}_2,$$

$$R^{m}_{33} = 4c^2 \operatorname{Re} \tilde{F}_2,$$

$$R^{m}_{23} = R^{m}_{32} = 2(1 + M^2) cs \operatorname{Re} \tilde{F}_2 / M, \tag{3.10}$$

where

$$\operatorname{Re}\tilde{F}_2 = -\frac{\alpha}{\pi}Q'^2\frac{M^2}{4\beta'}\ln\frac{1+\beta'}{1-\beta'},$$

$$\operatorname{Im}\tilde{F}_2 = -\alpha Q'^2 M^2/4\beta'.$$

This contribuion is one of the pure QED contributions of order α^3 to our process which produces non-zero polarization of a single τ. The polarization is of order $R^{\mathrm{m}}_{01}/R^0_{00}$ and numerically it is rather negligible. It should be noted however that this polarization only has components perpendicular to the production plane and is therefore parity conserving. A similar correction from the initial state vertex vanishes in the limit $m \to 0$.

At beam energies around 20 GeV the influence of the weak boson exchange cannot be neglected. We take it into account by including the $\gamma - Z_0$ interference in the form of a correction to the lowest order density matrix:

$$\tfrac{1}{4}\sum_{\lambda_i} M^0(M^Z)^* + M^Z(M^0)^*$$

$$= \tfrac{1}{2}QQ'e^4Z\{|\alpha_+\bar{\alpha}_+|2(v\tilde{v}+ca\tilde{a})+\alpha_+\bar{\alpha}_+2c(a\tilde{a}+cv\bar{v})$$

$$+(\alpha_+|\bar{\alpha}_+|+|\alpha_+|\bar{\alpha}_+)\,[(1+c^2)v\tilde{a}+2ca\tilde{v}]\}. \tag{3.11}$$

Here, v ($\tilde{v}$) and a ($\tilde{a}$) are the vector and axial coupling of the Z_0 to the electron (τ) and $Z = (1-M_Z^2/(p_1+p_2)^2)^{-1}$. We have taken in (3.11) the limit $M \to 0$ because the Z_0 contribution is important only in the energy range $E \gg m_\tau$. The contribution of the $\gamma - Z_0$ interference to the R-matrix reads

$$R^Z_{00} = R^Z_{33} = 2Z(QQ')^{-1}[(1+c^2)v\tilde{v}+2ca\tilde{a}],$$

$$R^Z_{11} = -R^Z_{22} = -2Z(QQ')^{-1}v\tilde{v}s^2,$$

$$R^Z_{03} = R^Z_{30} = 2Z(QQ')^{-1}[(1+c^2)v\tilde{a}+2ca\tilde{v}], \tag{3.12}$$

with all other elements equal to zero.

The longitudinal polarization of the τ resulting from the Z_0 exchange is given by the ratio:

$$R^Z_{03}/R^0_{00} = 2Z(QQ')^{-1}(v\tilde{a}+2ca\tilde{v}/(1+c^2)). \tag{3.13}$$

The total result for the R-matrix coming from the lowest order and from all corrections discussed in this Section is obtained by summing expressions (3.3), (3.7), (3.8), (3.10) and (3.12)

$$R^{\mathrm{soft}}_{ab} = R^{\mathrm{s}}_{ab}+R^{\mathrm{a}}_{ab}+R^{\mathrm{b}}_{ab}+R^{\mathrm{m}}_{ab}+R^{\mathrm{Z}}_{ab}. \tag{3.14}$$

4. Hard photon bremsstrahlung

The differential cross section for the process

$$\mathrm{e}^+(p_1)+\mathrm{e}^-(p_2) \to \tau^+(q_1)+\tau^-(q_2)+\gamma(k) \tag{4.1}$$

is defined by

$$d\sigma = \frac{\alpha^3(QQ')^2}{32\pi^2E^2}\,\frac{d^3q_1d^3q_2d^3k}{q_1^0q_2^0k^0}\,\delta^4(p_1+p_2-q_1-q_2-k)A(w_1, w_2), \tag{4.2}$$

where w_k are the polarization vectors of the $\tau^{\pm}(q_k)$ with $w_k \cdot q_k = 0$. The unpolarized cross section was given in Ref. [1]:

$$A(0, 0) = 2(A_{\text{ini}}+A_{\text{fin}}+A_{\text{int}}) \tag{4.3}$$

and the bilinear term in the decomposition

$$A(w_1, w_2) = A(0, 0)+\sum_{i,k=1}^{3} R_{ik}w_1^i w_2^k \tag{4.4}$$

contains a correlation matrix R_{ik} as in the lowest order. The absence of linear terms implies zero polarization for a single τ. Components of w_1^i and w_2^k are defined in certain rest frames of the τ^+ and τ^-, respectively. In this Section we shall concentrate on the calculation of all 32 spin amplitudes for the process (4.1) and we shall calculate R_{ik} from them. In Appendix C we give also a manifestly Lorentz invariant expression for $A(w_1, w_2)$ obtained with standard techniques.

In order to calculate spin amplitudes we introduce two reference frames with two orthogonal sets of basic vectors $\hat{e}_a$ and $\hat{e}'_a$ which are related to the particle momenta as follows:

$$\begin{aligned} k &= k(\hat{e}_0+\hat{e}_3), \quad & k &= y\bar{k}(\hat{e}'_0+\hat{e}'_3),\\ p_1 &= \hat{e}_0-\beta s_1\hat{e}_2+\beta c_1\hat{e}_3, \quad & q_1 &= y(\hat{e}'_0+vs_2\hat{e}'_2+vc_2\hat{e}'_3),\\ p_2 &= \hat{e}_0+\beta s_1\hat{e}_2-\beta c_1\hat{e}_3, \quad & q_2 &= y(\hat{e}'_0-vs_2\hat{e}'_2-vc_2\hat{e}'_3), \end{aligned} \tag{4.5}$$

where

$$\hat{e}_a \cdot \hat{e}_b = \hat{e}'_a \cdot \hat{e}'_b = g_{ab},$$

$$v = (1-\tilde{M}^2)^{1/2}, \quad \tilde{M} = M/y, \quad y = (1-k)^{1/2},$$

$$c_i = \cos\theta_i, \quad s_i = \sin\theta_i, \quad \bar{k} = k/y^2.$$

The reference system with basis $\hat{e}_a$ is a rotated c.m. system with the third axis along the photon momentum instead of the initial positive lepton momentum and we shall call it the PMK system. The second system will be referred to as the QMK system. They are related to each other by a simple Lorentz transformation;

$$\hat{e}_a = \Lambda_a{}^b\hat{e}'_b,$$

$$\{\Lambda_a{}^b\} = \begin{bmatrix} \bar{\gamma}, & 0, & 0, & \bar{\beta} \\ 0, & c_\varphi, & -s_\varphi, & 0 \\ 0, & s_\varphi, & c_\varphi, & 0 \\ \bar{\beta}, & 0, & 0, & \bar{\gamma} \end{bmatrix}, \tag{4.6}$$

where $c_\varphi = \cos\varphi$, $s_\varphi = \sin\varphi$, $\bar{\beta} = k/2y$, $\bar{\gamma} = (2-k)/2y$. The momenta of all five particles in (4.1) may be expressed using the four variables $k \in (k_0, 1-M^2)$, $\theta_i \in (0, \pi)$, $\varphi \in (0, 2\pi)$. The same variables are used to parametrize the phase space integral and to simulate M. C. events. For the latter purpose the fifth variable — the overall azimuthal angle around beam axis is also used. The spins of the initial fermions λ_i will be projected on $\vec{\hat{e}}_3$ in PMK and the spins α_i of the final fermions on $\vec{\hat{e}}'_3$ in QMK. The $\tau^\pm$ rest frames $\hat{e}_a^\pm$ used to define $\vec{w}_n$ in (4.4) are then obtained from QMK by a θ_2-rotation and a boost along $\vec{q}_1$ or $\vec{q}_2$. More precisely

$$\hat{e}_1^\pm = \hat{e}'_1, \quad \hat{e}_2^\pm = c_2\hat{e}'_2 - s_2\hat{e}'_3,$$

$$\hat{e}_3^\pm = (\pm v\hat{e}'_0 + s_2\hat{e}'_2 + c_2\hat{e}'_3)/\tilde{M}. \tag{4.7}$$

The hard bremsstrahlung spin amplitudes may be written in the following form:

$$M_{\lambda_i\alpha_i\gamma} = iUe(T^{\text{ini}}_{\lambda_i\alpha_i\gamma} + T^{\text{fin}}_{\lambda_i\alpha_i\gamma})$$

$$= U\left\{\frac{ieQ}{(q_1+q_2)^2}\tilde{V}_{\alpha_i\mu}H^\mu_{\lambda_i\gamma} + \frac{ieQ'}{(p_1+p_2)^2}V_{\lambda_i\mu}\tilde{H}^\mu_{\alpha_i\gamma}\right\}, \tag{4.8}$$

where the vector vertices

$$V = 2[|\lambda_+|\hat{e}_1 + i\lambda_+(c_1\hat{e}_2 + s_1\hat{e}_3)],$$

$$\tilde{V} = 2y[|\alpha_+|\hat{e}'_1 - i\alpha_+(c_2\hat{e}'_2 - s_2\hat{e}'_3) - \tilde{M}\alpha_-(s_2\hat{e}'_2 + c_2\hat{e}'_3)] \tag{4.9}$$

are taken from Appendix A and the bremsstrahlung parts

$$H^\mu_{\lambda_i\gamma} = \frac{-1}{2k\cdot p_1}\bar{v}(p_1\lambda_1)\not{\hat{e}}_\gamma(-\not{p}_1 + \not{k} + m)\gamma^\mu u(p_2\lambda_2)$$

$$- \frac{1}{2k\cdot p_2}\bar{v}(p_1\lambda_1)\gamma^\mu(\not{p}_2 - \not{k} + m)\not{\hat{e}}_\gamma u(p_2\lambda_2),$$

$$\tilde{H}^\mu_{\alpha_i\gamma} = \frac{1}{2k\cdot q_1}\bar{u}(q_2\alpha_2)\gamma^\mu(-\not{q}_1 - \not{k} + M)\not{\hat{e}}_\gamma v(q_1\alpha_1)$$

$$+ \frac{1}{2k\cdot q_2}\bar{u}(q_2\alpha_2)\not{\hat{e}}_\gamma(\not{q}_2 + \not{k} + M)\gamma^\mu v(q_1\alpha_1), \tag{4.10}$$

are calculated in Appendix D. The polarization vectors of the bremsstrahlung photon are chosen to be $\varepsilon_1 = \hat{e}_1$, $\varepsilon_2 = \hat{e}_2$, $\gamma = 1, 2$ or $\varepsilon_{1'} = \hat{e}'_1$, $\varepsilon_{2'} = \hat{e}'_2$, $\gamma = 1', 2'$. The Lorentz transformation (4.6) gives the relation between them. Neglecting terms which do not contribute to the cross section in the limit $m \to 0$, we have

$$H_1 = \frac{2}{m^2 + s_1^2}\{(|\lambda_+|s_1 - im|\lambda_-|)\hat{e}_2 - (i\lambda_+ s_1 - mc_1\lambda_-)c_1\hat{e}_1\},$$

$$H_2 = \frac{2}{\bar{\beta}(m^2+s_1^2)}\{(|\lambda_+|\bar{\gamma}s_1+im|\lambda_-|\bar{\beta})\hat{e}_1+(i\lambda_+\bar{\gamma}s_1+mc_1\lambda_-\bar{\beta})(c_1\hat{e}_2+\bar{\gamma}^{-1}s_1\hat{e}_3')\},$$

$$\tilde{H}_{1'} = \frac{2}{\tilde{M}^2+v^2s_2^2}\{vs_2[-|\alpha_+|\hat{e}_2'-i\alpha_+c_2\hat{e}_1']+i\tilde{M}|\alpha_-|\hat{e}_2'+\tilde{M}\alpha_-vc_2^2\hat{e}_1'\},$$

$$\tilde{H}_{2'} = \frac{2}{\bar{\beta}(\tilde{M}^2+v^2s_2^2)}\{vs_2[|\alpha_+|\bar{\gamma}\hat{e}_1'-i\alpha_+(\bar{\gamma}c_2\hat{e}_2'-s_2\hat{e}_3)]$$

$$-i\tilde{M}|\alpha_-|\bar{\beta}\hat{e}_1'+\tilde{M}\alpha_-v[(\bar{\beta}-\bar{\gamma}s_2^2)\hat{e}_2'-s_2c_2\hat{e}_3]\}. \tag{4.11}$$

It should be noted that both H and $\tilde{H}$ are manifestly gauge invariant i.e. $H_\gamma^\mu(q_1+q_2)_\mu = \tilde{H}_\gamma^\mu(p_1+p_2)_\mu = 0$.

In the soft photon limit $k \to 0$ both H_1 and $\tilde{H}_{1'}$ are negligible and we have

$$H_2 \cdot \tilde{V} = \frac{2s_1}{m^2+s_1^2} V \cdot \tilde{V},$$

$$\tilde{H}_{2'} \cdot V = \frac{2\beta' s_2}{M^2+\beta'^2 s_2^2} V \cdot \tilde{V}. \tag{4.12}$$

Even if it is not immediately obvious, both quantities in Eq. (4.12) are proportional to the same product $V \cdot \tilde{V}$ as the lowest order amplitude in Eq. (2.1). The apparent dissimilarity results from the different definitions of the axes which are transverse to the spin quantization axis.

The formulae for the spin amplitudes are now obtained by substituting (4.11) and (4.9) into (4.8);

$$T_\gamma^{\text{ini}} = \frac{Q}{y\bar{\beta}(m^2+s_1^2)}\{(|\lambda_+|s_1-im|\lambda_-|\xi_\gamma)(f_{11}^\gamma|\alpha_+|+f_{12}^\gamma i\alpha_+ +f_{13}^\gamma i|\alpha_-|$$

$$+f_{14}^\gamma\alpha_-)+(i\lambda_+s_1-m\lambda_-\xi_\gamma)(f_{21}^\gamma|\alpha_+|+f_{22}^\gamma i\alpha_+ +f_{23}^\gamma i|\alpha_-|+f_{24}^\gamma\alpha_-)\},$$

$$T_\gamma^{\text{fin}} = \frac{Q'}{\bar{\beta}(M^2+v^2s_2^2)}\{|\lambda_+|(g_{11}^\gamma|\alpha_+|+g_{12}^\gamma i\alpha_+ +g_{13}^\gamma i|\alpha_-|+g_{14}^\gamma\alpha_-)$$

$$+i\lambda_+(g_{21}^\gamma|\alpha_+|+q_{22}^\gamma i\alpha_+ +g_{23}^\gamma i|\alpha_-|+g_{24}^\gamma\alpha_-), \tag{4.13}$$

where $\xi^\gamma = c_1, -c_1\bar{\beta}/\bar{\gamma}$ for $\gamma = 1, 2$ respectively and the coefficients f_{ik}^γ and g_{ik}^γ are listed in Table II. Note that the index γ is different in the Table II for f_{ik}^γ and for g_{ik}^γ. Before we add the amplitudes for initial state and final state bremsstrahlung we have to rotate one of them. For example,

$$g_{ik}^1 = c_\varphi g_{ik}^{1'} - s_\varphi g_{ik}^{2'}, \qquad g_{ik}^2 = s_\varphi g_{ik}^{1'} + c_\varphi g_{ik}^{2'}. \tag{4.14}$$

TABLE II

The coefficients f^{γ}_{ik} and g^{γ}_{ik} in the formula (4.13) for hard photon bremsstrahlung amplitudes

j	1	2	3	4
f^{1}_{1j}	$-\bar{\beta}s_{\varphi}$	$\bar{\beta}c_2c_{\varphi}$	0	$\tilde{M}\bar{\beta}s_2c_{\varphi}$
f^{1}_{2j}	$\bar{\beta}c_1c_{\varphi}$	$\bar{\beta}c_1c_2s_{\varphi}$	0	$\tilde{M}\bar{\beta}c_1s_2s_{\varphi}$
f^{2}_{1j}	$-\bar{\gamma}c_{\varphi}$	$-\bar{\gamma}c_2s_{\varphi}$	0	$-\tilde{M}\bar{\gamma}s_2s_{\varphi}$
f^{2}_{2j}	$-\bar{\gamma}c_1s_{\varphi}$	$\bar{\gamma}c_1c_2c_{\varphi}-s_1s_2$	0	$\tilde{M}(\bar{\gamma}c_1s_2c_{\varphi}+s_1c_2)$
$g^{1'}_{1j}$	$-\bar{\beta}vs_2s_{\varphi}$	$\bar{\beta}vs_2c_2c_{\varphi}$	$\tilde{M}\bar{\beta}s_{\varphi}$	$-\tilde{M}\bar{\beta}vc_2^2c_{\varphi}$
$g^{1'}_{2j}$	$\bar{\beta}vs_2c_1c_{\varphi}$	$\bar{\beta}vs_2c_2c_1s_{\varphi}$	$-\tilde{M}\bar{\beta}c_1c_{\varphi}$	$-\tilde{M}\bar{\beta}vc_2^2c_1s_{\varphi}$
$g^{2'}_{1j}$	$-\bar{\gamma}vs_2c_{\varphi}$	$-\bar{\gamma}vs_2c_2s_{\varphi}$	$\tilde{M}\bar{\beta}c_{\varphi}$	$-\tilde{M}v(\bar{\gamma}s_2^2-\bar{\beta})s_{\varphi}$
$g^{2'}_{2j}$	$-\bar{\gamma}vs_2c_1s_{\varphi}$	$vs_2(\bar{\gamma}c_1c_2c_{\varphi}-s_1s_2)$	$\tilde{M}\bar{\beta}c_1s_{\varphi}$	$\tilde{M}v((\bar{\gamma}s_2^2-\bar{\beta})c_1c_{\varphi}+s_2c_2s_1)$

If one is interested only in the case of unpolarized beam particles then the following replacement may be introduced;

$$(|\lambda_+|s_1-im|\lambda_-|\xi_{\gamma})f^{\gamma}_{1k} \Rightarrow |\lambda_+|\,(s_1^2+m^2\xi_{\gamma}^2)^{1/2}f^{\gamma}_{1k} = |\lambda_+|f'^{\gamma}_{1k},$$

$$(i\lambda_+s_1-m\lambda_-\xi_{\gamma})f^{\gamma}_{2k} \Rightarrow i\lambda_+(s_1^2+m^2\xi_{\gamma}^2)^{1/2}f^{\gamma}_{2k} = i\lambda_+f'^{\gamma}_{2k}. \tag{4.15}$$

In that case the spin amplitudes may be written in a more compact form:

$$\begin{aligned} T_{\lambda_i\alpha_i\gamma} &= T^{\mathrm{ini}}_{\lambda_i\alpha_i\gamma}+T^{\mathrm{fin}}_{\lambda_i\alpha_i\gamma} \\ &= |\lambda_+|\,(h^{\gamma}_{11}|\alpha_+|+h^{\gamma}_{12}i\alpha_++h^{\gamma}_{13}i|\alpha_-|+h^{\gamma}_{14}\alpha_-) \\ &+i\lambda_+(h^{\gamma}_{21}|\alpha_+|+h^{\gamma}_{22}i\alpha_++h^{\gamma}_{23}i|\alpha_-|+h^{\gamma}_{24}\alpha_-), \end{aligned} \tag{4.16}$$

where

$$h^{\gamma}_{ik} = \frac{Q}{y\bar{\beta}'(m^2+s_1^2)}f'^{\gamma}_{ik}+\frac{Q'}{\bar{\beta}(\tilde{M}^2+v^2s_2^2)}g^{\gamma}_{ik}. \tag{4.17}$$

The matrix R_{ab} is calculated using the relations (A.9) from Appendix A:

$$\begin{aligned} R_{00} &= (1,1)+(2,2)+(3,3)+(4,4), \\ R_{11} &= -(1,1)+(2,2)-(3,3)+(4,4), \\ R_{22} &= (1,1)-(2,2)-(3,3)+(4,4), \\ R_{33} &= (1,1)+(2,2)-(3,3)-(4,4), \\ R_{12} &= 2[(1,2)+(3,4)], \quad R_{21} = 2[(1,2)-(3,4)], \\ R_{13} &= 2[(1,4)-(2,3)], \quad R_{31} = 2[(1,4)+(2,3)], \\ R_{23} &= 2[-(2,4)-(1,3)], \quad R_{32} = 2[-(2,4)+(1,3)], \end{aligned} \tag{4.18}$$

where $(k, l) = \sum_{\gamma,i} h_{ik}^{\gamma} h_{il}^{\gamma}$. In practice it is rather easy to do the transition from Table II to R_{ab} defined in Eqs. (4.17) numerically.

We have checked that the algebraic expression in terms of c_i, s_i and k obtained from the formula

$$A_{\text{fin}} = \frac{Q'^2}{2\beta^2(\tilde{M}^2 + v^2 s_2^2)^2} \sum_{\gamma,i,k} (g_{ik}^{\gamma})^2 \tag{4.19}$$

and from A_{fin} as defined in Ref. [1] agree. The same agreement was found for the initial state cross section

$$A_{\text{ini}} = \frac{Q^2}{2y^2\beta^2(m^2 + s_1^2)^2} \sum_{\gamma,i,k} (f_{ik}^{\prime\gamma})^2. \tag{4.20}$$

Another test was done numerically: We have compared R_{ab} obtained from the formulae given in the Appendix D with R_{ab} calculated from Eqs. (4.18) for a series of M.C. events. We have obtained good agreement also separately for every part like initial state, final state radiation and their interference.

5. *Numerical results*

In e^+e^- experiments the τ lepton is only observed through its decay products. The experimental sample of the $\tau^+\tau^-$ events is isolated using kinematical cuts even more complicated than for stable leptons.

In practice the influence of experimental cuts is taken into account by M. C. simulation. Furthermore QED radiative corrections to order α^3 change the total and differential cross section [2]. In the case of hard photon bremsstrahlung, M.C. simulation is again the most useful way to introduce QED corrections into the data analysis, see Refs. [3], [5] and [6]. Spin effects of the type discussed in this paper do not change the total cross section but they enhance the differential cross section in some parts of the phase space of the observed decay products and decrease it in other parts. When kinematical cuts are introduced the M.C. method is the best way to include such effects. Mass effects are hardly separable from spin effects and radiative corrections.

In our numerical calculations we shall estimate quantitatively effects resulting from spin correlations. Generally we expect that they will be stronger in the case of the lowest order than in order α^3 because the hard bremsstrahlung smears out asymmetries resulting from the spin effects. We shall investigate the influence of the radiative corrections on the energy and angular distributions of the decay products.

The effects of weak boson (Z_0) exchange are also discussed. We examine its influence on the charge asymmetry and c.m.s. energy distribution of the charged decay products of the τ. The energy distribution is modified in a characteristic way by τ polarization due to Z_0 exchange.

In our M.C. calculations we take for simplicity only the decays of the τ into one charged particle

$$\tau^{\pm}(q) \to \mathrm{f}^{\pm}(p_{\mathrm{f}}) + \text{neutrals}, \tag{5.1}$$

with the following decay probability distribution in the τ rest system:

$$\frac{dP(\tau^{\mp})}{d\Omega dx} = \frac{1}{4\pi} a(x)\,(1 \pm g(x)\vec{n}\cdot\vec{w}) = \frac{1}{4\pi} a(x)\,(1+\vec{h}^{(\mp)}\cdot\vec{w}), \tag{5.2}$$

where $x = 2E_f/M_\tau$, $\vec{n} = \vec{p}_f/|\vec{p}_f|$, $\vec{h}^{(\mp)} = \pm\vec{n}g(x)$ and $\vec{w}$ is the τ polarization vector in its rest frame. The functions $a(x)$ and $g(x)$ are listed in Table III for f = e, μ, π, ϱ.

TABLE III

Properties of the τ decays used in the Monte Carlo calculations. Functions $a(x)$ and $g(x)$ are defined in Eq. (5.2). Branching ratios are taken from Ref. [8]

Decay mode	Branching ratio	$a(x)$	$g(x)$	Comments
$\tau^- \to e^-\bar{\nu}_e\nu_\tau$ $\tau^- \to \mu^-\bar{\nu}_\mu\nu_\tau$	18% 18%	$2x^2(3-2x)\theta(1-x)$	$\frac{2x-1}{3-2x}$	$m_e = m_\mu = 0$
$\tau^- \to \rho^-\nu_\tau$	23%	$\delta(1+\rho^2-x)$	$\frac{1-2\varrho^2}{1+2\varrho^2} = 0.48$	$\varrho^2 = \left(\frac{m_\varrho}{m_\tau}\right)^2 = 0.175$
$\tau^- \to \pi^-\nu_\tau$	10%	$\delta(1-x)$	1	$m_\pi = 0$

The differential cross section for the process

$$\begin{aligned} e^+(p_1)+e^-(p_2) \to \tau^+(q_1)+\tau^-(q_2)+(\gamma(k)) \\ \qquad\qquad\qquad\qquad\quad \big\lfloor\!\to f^-(p_-)+\text{neutrals} \\ \qquad\qquad\qquad\qquad\quad \big\lfloor\!\to f^+(p_+)+\text{neutrals} \end{aligned} \tag{5.3}$$

is given by the formula

$$d\sigma = \Big(\sum_{a,b=0}^{3} r_{ab}h_a^{(+)}h_b^{(-)}\Big)d\sigma_{up}dP_+dP_-, \tag{5.4}$$

where $r_{ab} = R_{ab}/R_{00}$, $d\sigma_{up}$ is the spin summed/averaged differential cross section for $e^+e^- \to \tau^+\tau^-(\gamma)$ and $dP_\pm$ is the differential probability distribution for the decay of an unpolarized $\tau^\pm$, i.e. $dP = a(x)d\Omega/4\pi$. Vectors $\vec{h}^{(\pm)}$ are supplemented with the components $h_0^{(+)} = h_0^{(-)} = 1$ in order to make formula (5.4) more compact. All spin effects are coming from the first factor in Eq. (5.4). The formal proof of the formula (5.4) is given at the end of Appendix A. For some comments see also Ref. [7].

The M.C. simulation algorithm consists of the following steps:

1) The four-vectors of $\tau^+\tau^-(\gamma)$ are generated according to the spin summed/averaged differential cross section $d\sigma_{up}$ using methods described in Refs. [1] and [9]. The joint density matrix r_{ab} is calculated.

2) For each τ the decay is simulated, i.e. x and $\vec{n}$ are chosen in the τ rest frame assuming an unpolarized τ. The basis in which $\vec{n}$ is defined is described in Sections 2 ($e^+e^- \to \tau^+\tau^-$) and 4 ($e^+e^- \to \tau^+\tau^-\gamma$). These bases are used in all amplitude calculations. Vectors $\vec{h}^{(+)}$ and $\vec{h}^{(-)}$ are calculated in the corresponding rest systems.

3) The weight

$$w = \tfrac{1}{2} \sum_{a,b=0}^{3} r_{ab}(q_1, q_2) h_a^{(+)}(p_+) h_b^{(-)}(p_-) \tag{5.5}$$

is calculated and compared with the uniform random number $r \in (0, 1)$. The weight obeys the inequality $0 \leqslant w \leqslant 1$. When $w < r$ the event as a whole is accepted, otherwise it is rejected. On the average half of the events are rejected.

4) For the accepted event the momenta of the decay products are transformed from the respective τ rest systems to the c.m. system.

We would like to stress that the algorithm is built in such a way that the decay mechanism may be easily changed, modified and improved without any changes in the τ pair production part.

Before we come to the numerical results let us try to understand the decay correlations in the simplest example of both τ's decaying into $\pi\nu$ in the lowest order and in the limit $M \to 0$. The correlation between the pion momenta are controlled by the weight

$$w = \tfrac{1}{2}\left[1 - \cos\theta_1 \cos\theta_2 + \sin\theta_1 \sin\theta_2 \cos(\varphi_1 + \varphi_2) \frac{s^2}{1+c^2}\right], \tag{5.6}$$

where the direction of the π in the corresponding τ rest system is $\vec{n}_i = (\sin\theta_i \cos\varphi_i, \sin\theta_i \sin\varphi_i, \cos\theta_i)$, $i = 1, 2$. Averaging over θ, φ_i and relating θ_i to the π c.m. energy $y_i \in (0, 1)$ we obtain

$$\frac{1}{\sigma} \frac{d\sigma}{dy_1 dy_2} = 1 + (2y_1 - 1)(2y_2 - 1). \tag{5.7}$$

As we see we have more fast-fast and slow-slow pairs than fast-slow pairs. The longitudinal asymmetry A_{long} defined as

$$A_{\text{long}} = \Big(\int_0^{\frac{1}{2}}\int_0^{\frac{1}{2}} + \int_{\frac{1}{2}}^{1}\int_{\frac{1}{2}}^{1} - \int_0^{\frac{1}{2}}\int_{\frac{1}{2}}^{1} - \int_{\frac{1}{2}}^{1}\int_0^{\frac{1}{2}} dy_1 dy_2\Big) \Big/ \int_0^1\int_0^1 dy_1 dy_2 \tag{5.8}$$

is equal to 1/4 in this case. The same result is obtained from M.C. calculations, see Table IV.

The decay of each τ into $\pi\nu$ is rather rare as can be seen from the branching ratios in Table III. In the more realistic case of the τ decaying either into $\pi\nu$ or $\rho\nu$ we obtain an A_{long} around 1/10 in the lowest order, see Table IV. The reason is that the ρ-decay is about twice less sensitive to the τ polarisation ($g_\varrho = 0.48$) than the π-decay ($g_\pi = 1$) as indicated in Table III. The purely leptonic decays are even less sensitive as a spin analyzer, $g_{e,\mu} = \int a(x)g(x)dx = 0.17$.

In Table IV we show the M.C. results for A_{long} at two beam energies, $E = 5$ GeV and $E = 20$ GeV. We compare results from lowest order and $O(\alpha^3)$ calculations, with and without spin for each energy, see Table IV.

We first consider the spinless case. If only the decay $\tau \to \pi\nu$ is considered, $A_{\text{long}} = 0$ in the lowest order as expected. Including also the decay $\tau \to \varrho\nu$, due to the finite ϱ mass, A_{long} no longer vanishes even in the lowest order. Going to $O(\alpha^3)$ a small positive correla-

TABLE IV

Longitudinal and transverse asymmetries defined in Eqs. (5.8) and (5.10), calculated using samples of 10^5 M.C. events at beam energies $E = 5$ GeV and $E = 20$ GeV. Asymmetries are given in percents. Statistical errors are 0.3% for A_{long} and 0.7% for A_{tran}. In the calculation of A_{tran} we use the cut-off on the energies of the decay products $|1/2 - y_i| < 0.2$. The Z_0 contribution is not included

	E	Decay mode	$O(\alpha^2)$		$O(\alpha^3)$	
			spin off	spin on	spin off	spin on
A_{long}	20 GeV	$\pi\nu$	−0.2	24.4	5.4	25.2
		$\pi\nu+\rho\nu$	2.2	12.2	4.8	12.7
	5 GeV	$\pi\nu$	0.2	22.0	2.7	22.2
		$\pi\nu+\rho\nu$	2.2	11.3	3.1	11.7
A_{tran}	20 GeV	$\pi\nu$	1.1	24.1	−19.2	−4.9
		$\pi\nu+\rho\nu$	1.4	9.4	−20.6	−14.5
	5 GeV	$\pi\nu$	1.6	19.6	−5.2	11.3
		$\pi\nu+\rho\nu$	0.2	6.8	−6.4	−0.6

tion is observed, because hard bremsstrahlung tends to decrease the c.m.s. pion energies. At the lower beam energy ($E = 5$ GeV) the influence of hard bremsstrahlung is weaker as compared to $E = 20$ GeV, leading to smaller values of A_{long} in the $O(\alpha^3)$ results. Spin effects on the other hand do not change A_{long} substantially going from $E = 5$ GeV to $E = 20$ GeV.

When spin effects are switched on, the difference between A_{long} calculated with and without spin remains similar in both the lowest order and in $O(\alpha^3)$ results. The value of A_{long} is increased by spin effects by about 20–25% in the case of each τ decaying into $\pi\nu$ and by 7–12% in the case of each τ decaying into $\pi\nu$ or $\varrho\nu$. These effects are seen also clearly in Fig. 1 where we plot $d\sigma/(\sigma dy_1 dy_2)$. This distribution is uniform in the lowest order spinless case. In Fig. 1a we show $d\sigma/(\sigma dy_1 dy_2)$ in $O(\alpha^3)$ without spin effects. As compared to lowest order the distribution is enhanced in the low y_i region due to hard bremsstrahlung. In Fig. 1b we give the $O(\alpha^3)$ result for the same distribution with spin effects included. The net decrease of $d\sigma/(\sigma dy_1 dy_2)$ in regions around $(y_1, y_2) = (0, 1), (1, 0)$ (slow-fast configurations) and enhancements in region $(y_1, y_2) = (0, 0), (1, 1)$ (fast-fast, slow-slow configurations) are due to spin effects and they are also the source of the 20% increase of A_{long} in Table IV.

The other type of spin-induced correlations are the correlations between the transverse momenta of the decay products. They are strongest when both τ's decay in the transverse direction, i.e. $\theta_i = \pi/2$. For the lowest order both τ's decaying into $\pi\nu$ the correlation factor reads

$$w = \tfrac{1}{2}\left(1 + \cos(\varphi_1 + \varphi_2)\,\frac{s^2}{1+c^2}\right), \tag{5.9}$$

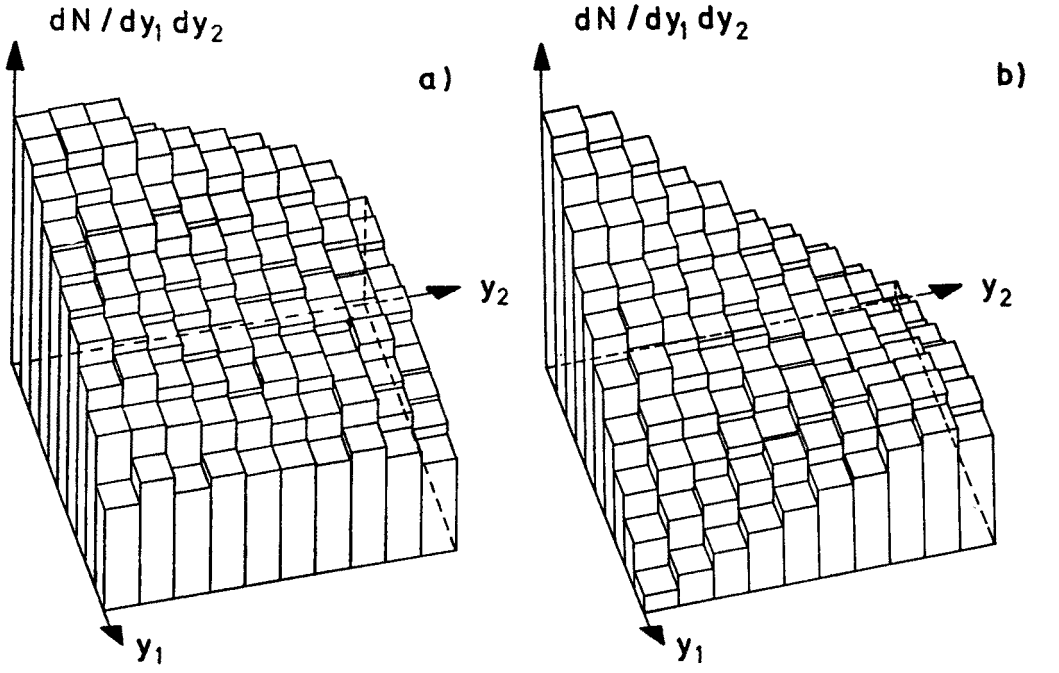

Fig. 1. The differential cross section $d\sigma/dy_1 dy_2$ (in arbitrary units) from $O(\alpha^3)$ QED calculations a) without and b) with spin effects included, at $E = 20$ GeV. Each τ decays into $\pi\nu$. The pion energies y_i are given in units of the beam energy E

where φ_i is the azimuthal angle of the pion momentum with respect to τ^+ c.m. momentum, for simplicity we assume $y_i = 1/2$. Since we do not observe the direction of the τ momentum directly we study asymmetry in the angle $\alpha \in (0, \pi/2)$ defined in c.m.s. as the angle between the reaction plane $(\vec{p}_1, \vec{p}_+)$ and the plane of decay products $(\vec{p}_+, \vec{p}_-)$. The two planes, as can be deducted from (5.9), tend to be orthogonal and we introduce the transverse asymmetry, defined as

$$A_{\text{tran}} = \left(\int_{\pi/4}^{\pi/2} - \int_{0}^{\pi/4} d\alpha\right) / \int_{0}^{\pi/2} d\alpha, \tag{5.10}$$

to measure the strength of the effect.

In Table IV, together with value of A_{long} we give also the M.C. results for A_{tran}. They are obtained imposing the condition $|y_i - 1/2| < 1/5$ which reduces the number of events (cross section) approximately by factor four. Comparing the results for A_{tran} from the lowest order and from $O(\alpha^3)$ calculations we find similar effects due to hard bremsstrahlung as for A_{long}. The net increase of A_{tran} due to spin correlations is varying from 20–25% in the case of the τ's decaying into $\pi\nu$ to 5–10% in the case of each τ decaying into $\pi\nu$ or $\varrho\nu$. This net spin effect in A_{tran} depends rather weakly on the beam energy.

In Fig. 2 the acollinearity distribution $d\sigma/d\zeta$ is shown for two beam energies $E = 5$ GeV and $E = 20$ GeV with and without $O(\alpha^3)$ radiative corrections. The acollinearity angle

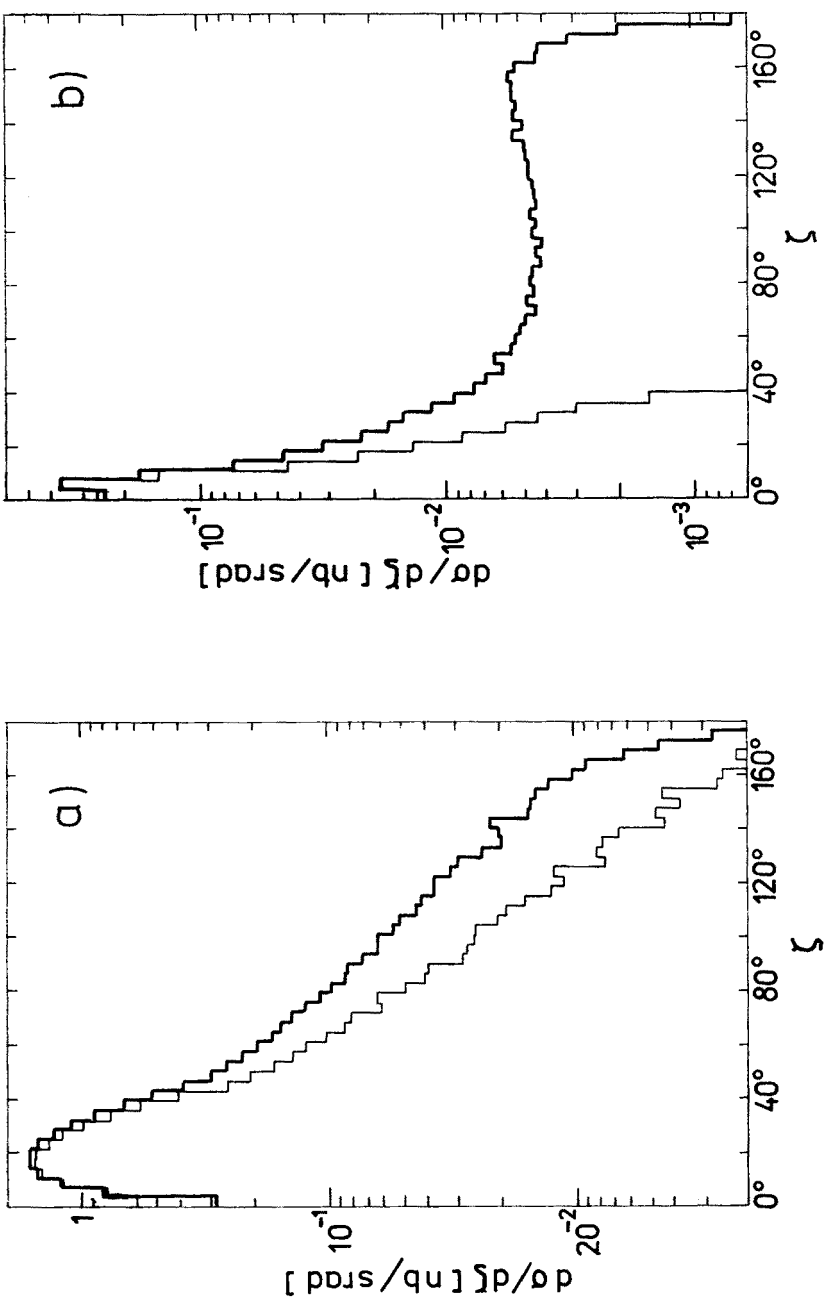

Fig. 2. The acollinearity distribution $d\sigma/d\zeta$ at the beam energy a) $E = 5$ GeV, b) $E = 20$ GeV. The acollinearity angle is defined between momenta of the charged decay products. Each τ decays either into $\pi\nu$ or $\rho\nu$ according to branching ratios and decay distributions from Table III. Fat and slim lines show $O(\alpha^3)$ and $O(\alpha^2)$ results

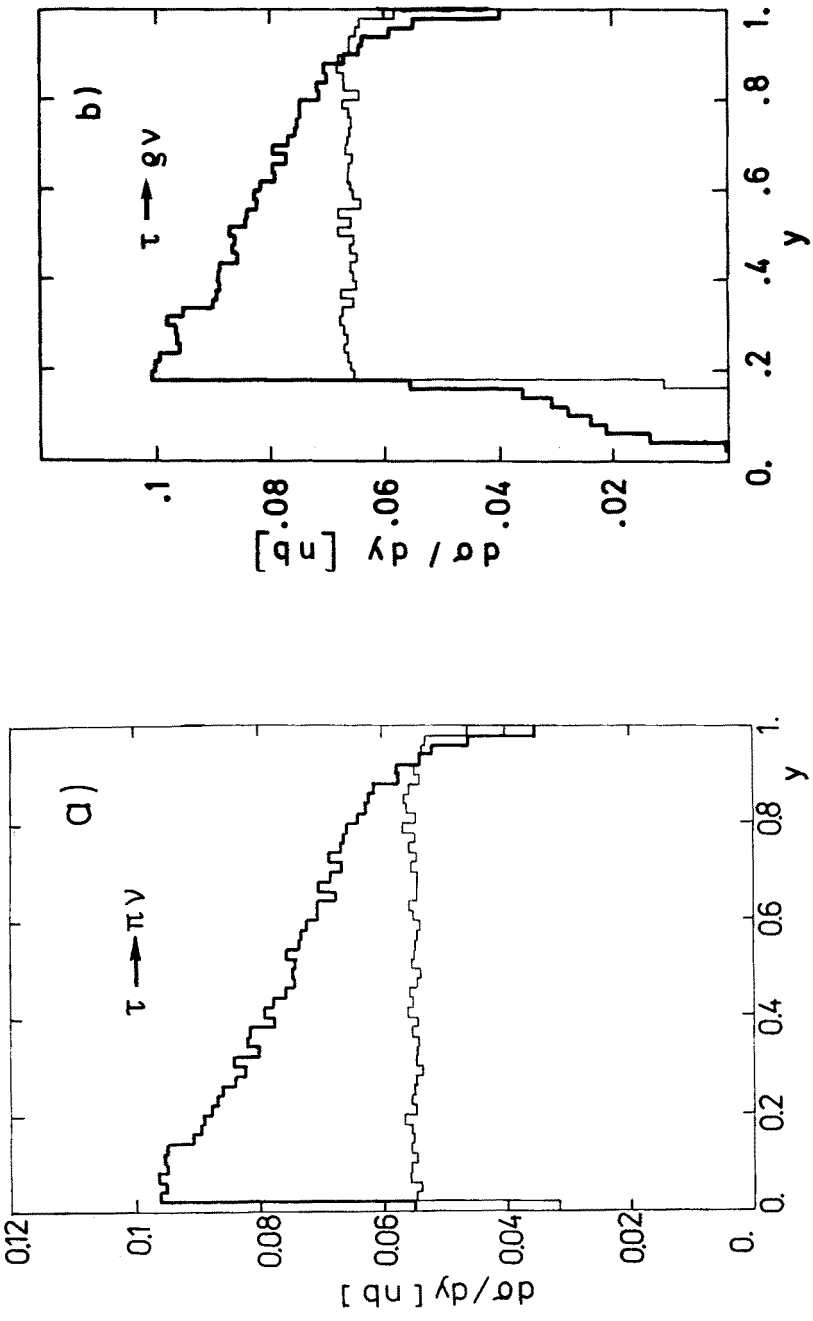
a)
τ → π ν
dσ/dy [nb]
0,12
0.1
0.08
0.06
0.04
0.02
0.
0.2
0.4
0.6
0.8
1.
y
b)
τ → ϱ ν
dσ / dy [nb]
.1
.08
.06
.04
.02
0.
.2
.4
.6
.8
1.
y

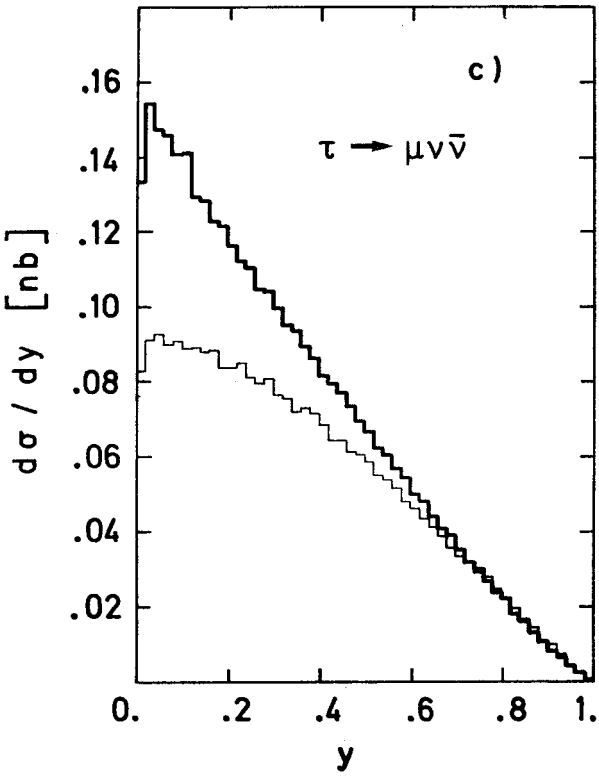

Fig. 3. The energy distribution $d\sigma/dy$ where y is energy (in units of E) of the charged decay product being a) π, b) ϱ, c) μ (or electron). Fat and slim curves show $O(\alpha^3)$ and $O(\alpha^2)$ QED results at the beam energy $E = 20$ GeV

$\zeta = \sphericalangle(\vec{p}_+, \vec{p}_-)$ is defined using the momenta of the charged decay products. Each τ is decaying into $\pi\nu$ or $\varrho\nu$. At both energies the increase of $d\sigma/d\zeta$ at large acollinearity, see Fig. 2, is due to hard bremsstrahlung and, as expected, is larger at the higher beam energy.

In Fig. 3 we show the energy distribution $d\sigma/dy$ for the charged decay products from the decays $\tau \to \pi\nu$, $\varrho\nu$, $\mu\nu\bar{\nu}$ at $E = 20$ GeV. For each decay mode the two curves represent the result of the lowest order and $O(\alpha^3)$ calculations. For all three decays in $O(\alpha^3)$ the energy distribution is increased at low y as compared to the lowest order. As was already pointed out this increase is due to hard bremsstrahlung. The gap at low y in $d\sigma/dy$ for $\tau \to \varrho\nu$ (Fig. 3b) is caused by finite mass of the ϱ and is partly smeared out when hard bremsstrahlung is switched on.

In Figs. 1, 2, 3 we did not include Z_0 contribution because we have been discussing so far pure QED effects. But even if Z_0 was included (with standard model coupling constants) these distributions would not change noticeably. At beam energies around 20 GeV we expect to observe two phenomena related to Z_0 exchange. One is charge asymmetry in the differential cross section $d\sigma/d\cos\theta d\varphi$ for the charged decay products and the second is polarization of the τ.

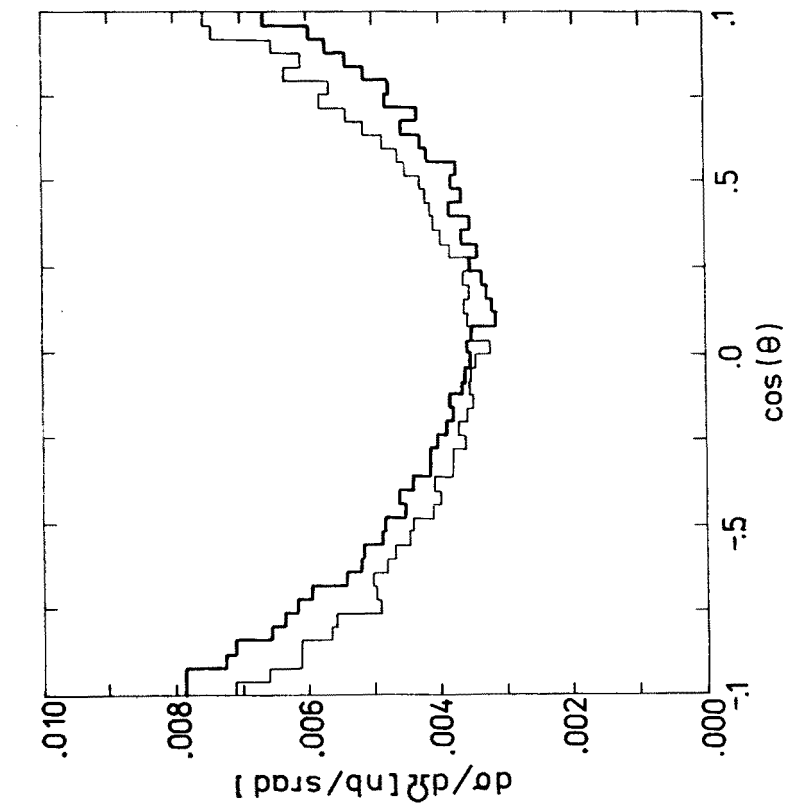

Fig. 4

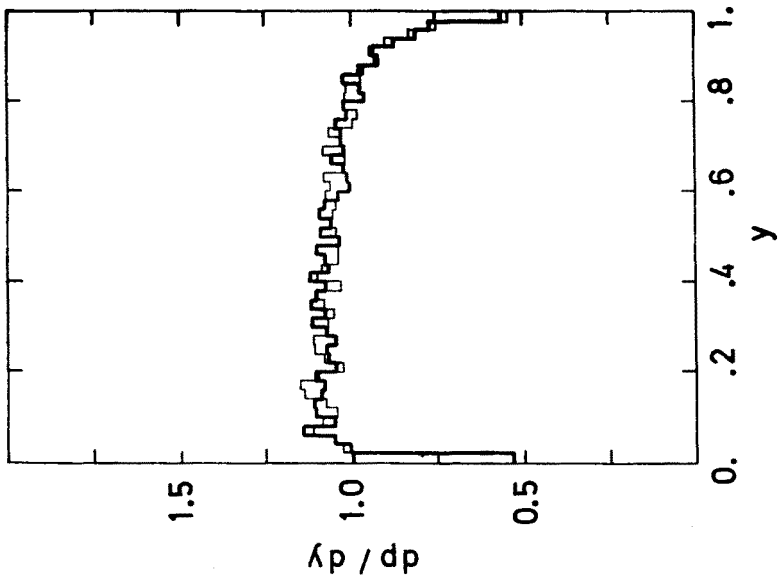

Fig. 5

Fig. 4. The angular distribution $d\sigma/d\Omega$ for charged decay products at $E = 20$ GeV. Each τ decays into $\pi\nu$ or $\rho\nu$. The visible energy and acollinearity cut-offs, $y_1 + y_2 > 0.4$, $\zeta < 30°$, are employed to select events. The slim curve represents the $O(\alpha^3)$ QED result and the fat curve includes in addition the contribution from Z_0 exchange

Fig. 5. The energy distribution $d\sigma/dy$ for the π^+ meson in the forward hemisphere (fat line) and in the backward hemisphere (slim line) at $E = 20$ GeV with an acollinearity cut-off $\zeta < 45°$. The distributions are normalized to unity. $O(\alpha^3)$ QED corrections and Z_0-exchange with standard GWS [11] coupling constants for $\sin^2\theta_W = 0.23$ are included

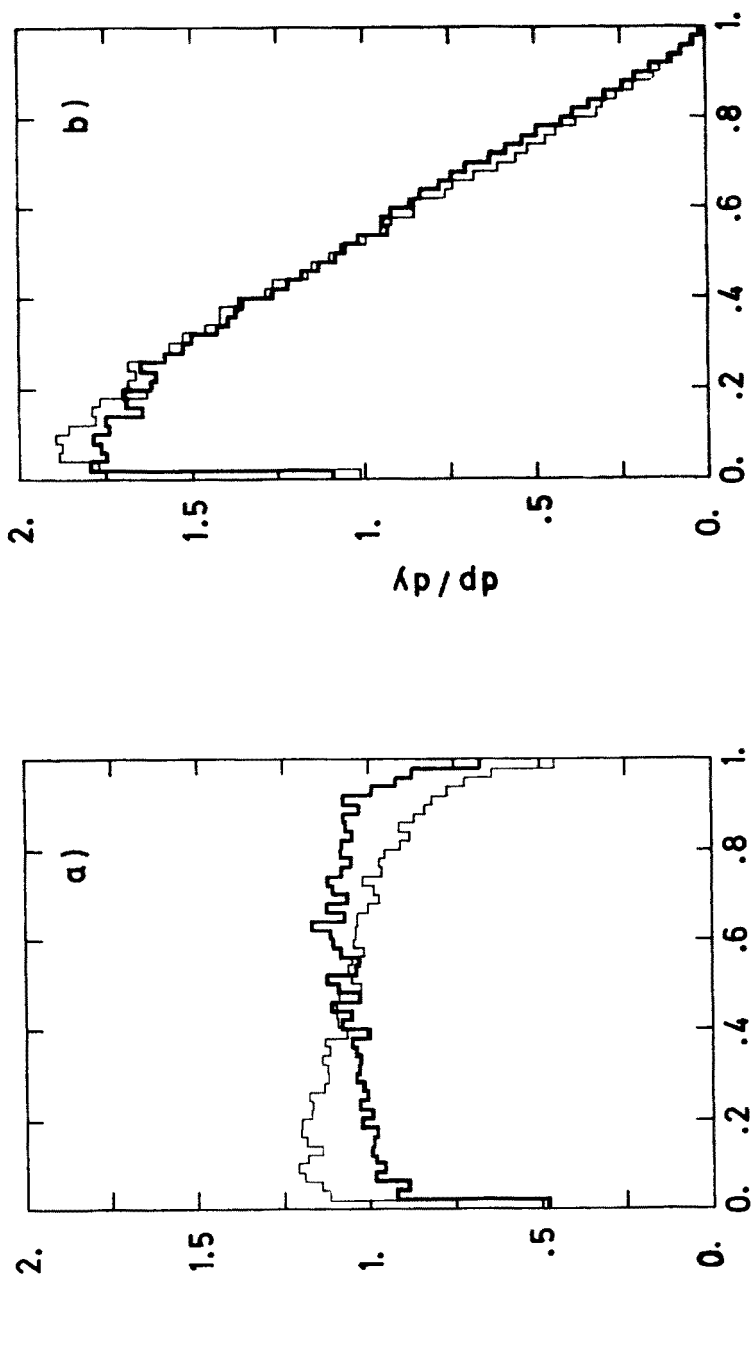

Fig. 6. The same energy distribution as in Fig. 5 for two decays a) $\tau \to \pi\nu$, b) $\tau \to \mu\nu\bar{\nu}$. In order to enhance τ polarisation the coupling constants are chosen in the following way: $\tilde{v} = \tilde{a} = \tilde{a}_{\mathrm{GWS}}$

In our discussion on the charged asymmetry we limit ourselves to the decays $\tau \to \pi\nu, \varrho\nu$. The scattering angle θ is defined as the angle between e^+ and π^+ or ϱ^+. Since QED $O(\alpha^3)$ radiative corrections also contribute to the charged asymmetry one has to subtract QED effects in order to obtain pure electroweak contribution.

The angular dependence of the differential cross section $d\sigma/d\Omega$ is shown in Fig. 4. We employed typical experimental cuts to select the event sample, i.e. $\zeta < 30°$ and visible energy > 0.2 ($y_1 + y_2 > 0.4$). The slim curve represents pure QED $O(\alpha^3)$ result and the fat curve includes in addition $\gamma - Z_0$ interference in the way described in Section 3. The values of the weak coupling constant and the Z_0 mass are chosen as in the standard GWS model [11] with $\sin^2\theta_W = 0.23$. The angular asymmetry which is slightly positive in the case of pure QED $O(\alpha^3)$ ($+1.7\%$) changes to negative value (-10.6%) after Z_0 exchange is included.

Longitudinal τ-polarization resulting from Z_0 exchange depends on $\cos\theta$, see Eq. (3.13). Since the c.m. energy distribution $d\sigma/dy$ of the charged decay products is sensitive to the polarization of the τ we determine this distribution in the forward and backward hemisphere separately. In Fig. 5 we show these two energy distributions for $\tau \to \pi\nu$ using coupling constants given by the standard GWS model with $\sin^2\theta_W = 0.23$. Both curves are normalised to unity, and the cut-off $\zeta < 45°$ was used in the calculations. There is no visible effect due to the fact that $\sin^2\theta_W$ is close to 0.25 (vector coupling constant $\tilde{v} \cong 0$). To show how such effect might look like we change $\tilde{v}$ for the final lepton τ, setting $\tilde{v} = \tilde{a}_{GWS}$. The result, again for $\tau \to \pi\nu$, is shown in Fig. 6a where $d\sigma/dy$ differs for two hemispheres. A similar effect is seen in Fig. 6b where we show the result for $\tau \to \mu\nu\bar{\nu}$ with the same choice of coupling constants in order to increase the polarization of the τ. The effect is weaker than for $\pi\nu$ decay, but still visible.

6. *Conclusions*

In this article we investigate the electron-positron annihilation into a pair of heavy unstable fermions (τ leptons) in QED to order α^3. In the numerical calculations we include also the decay of the final fermions. Our work is relevant first of all to $e^+e^- \to \tau^+\tau^-$ from threshold to $\sqrt{s} \simeq 40$ GeV. In this process spin effects in the final state cannot be neglected even in the case of unpolarized incident beams because the parity violating decay of τ is sensitive to its spin.

We calculated the complete set of QED spin amplitudes to $O(\alpha^3)$ both for virtual corrections and for soft/hard bremsstrahlung for the reaction $e^+e^- \to \tau^+\tau^-(\gamma)$. The mass of the final fermion is kept through the calculations. The contribution from an intermediate boson Z_0 is also included in the lowest order in the low energy approximation ($s \ll M_Z^2$).

To obtain the numerical results we use the direct M.C. simulation of the process including the decay. There are various reasons to use the M.C. method:

a) It was found [2, 3, 5] that the M.C. method is the best suited to investigate the effects of hard bremsstrahlung.

b) The τ lepton cannot be observed directly but only through its decay products. Thus

the production process cannot be isolated and discussed separately from the decay. The decay of τ is easily included in M.C. simulation.

c) Spin effects cannot be eliminated from the process because one is not able to measure the τ momentum and the decay of τ is sensitive to its spin. We found an easy way to include the polarization of the τ and other spin effects in the M.C. simulation.

d) In a typical experiment a sample of $\tau^+\tau^-$ events is isolated using a complicated set of kinematical cuts. The M.C. simulation provides an easy and natural way to control the influence of these cuts.

In our M.C. algorithm the connection between the production and decay is made in terms of spin density matrices which we calculate from the spin amplitudes. This method allows us to keep separate the production and the decay parts of the M.C. algorithm. One may change easily the decay matrix element without any intervention in the production part.

In the examples of the numerical results based on the M.C. calculations we show the influence of radiative corrections including hard bremsstrahlung, mass effects, spin effects and electroweak effects due to Z_0 exchange on the spectra of the charged decay products. We limit ourselves to the decays of the τ into one charged particle such as $\tau \to e\bar{\nu}\nu$, $\mu\bar{\nu}\nu$, $\pi\nu$, $\varrho\nu$. The energy and angular distributions show typical QED radiative corrections of order 10–20% in the energy range $\sqrt{s}$ from 10 to 40 GeV.

We concentrate on the effects induced by spin correlations in the decay of the two τ's in lowest order and in $O(\alpha^3)$. We find that the momenta of the decay products from two τ leptons are correlated in a specific way and that the magnitude of the correlations depends on the decay mode. In the case of $\tau \to \pi\nu$, $\varrho\nu$ the spin effects can be as important as the radiative corrections.

The effect of the Z_0 exchange is also taken into account in the calculations in the form of the $\gamma - Z_0$ interference.

In our numerical examples we determine the charge asymmetry in the angular distribution of the τ decay products arising from Z_0-exchange. We also discuss the effects due to τ-polarization induced by weak neutral currents.

It should be remarked that there exist two natural future extensions of this work, i.e. the inclusion of beam polarization and of the Z_0 in the resonance form. It will be rather straightforward to include the beam polarization because we already calculated the spin amplitudes and only the transition from the spin amplitudes to the density matrices has to be changed. The inclusion of the Z_0 boson in the full resonance form together with QED corrections to Z_0 exchange can be done relatively easily for light final fermions like τ leptons because the approximation $m_\tau \ll M_Z$ can be used. It would be more difficult to extend our calculations to the case of heavy fermions with the masses compatible to the Z_0 mass.

One of authors (S.J.) wishes to acknowledge the warm hospitality of the Lorentz Institute, Leiden, and of the Max-Planck-Institut für Physik und Astrophysik, München, where the part of the work presented here was done. Helpful discussions with drs. C. Kiesling, F. Berends and R. Kleiss are also acknowledged.

APPENDIX A

In this Appendix we give some formulae which relate products of two spinors with well-defined spin projections to other quantities like scalars, vectors etc. and to projection operators $\Lambda_{\pm}$.

Consider a pair of two fermions with mass m and c.m. momenta $p_1 = (1, 0, 0, \beta)$, $p_2 = (1, 0, 0, -\beta)$. We shall express the vertices

$$V_{J,\lambda_1\lambda_2} = \bar{v}(p_1\lambda_1)\Gamma_J u(p_2\lambda_2), \tag{A.1}$$

where $\Gamma_J = \{1, \gamma_\mu, [\gamma_\mu\gamma_\nu], \gamma_5\gamma_\mu, \gamma_5\}$, $J = $ S, V, T, A, P in terms of four basic c.m. system vectors $(\hat{e}_\alpha)^\mu = \delta^\mu_\alpha$, $\hat{e}_\alpha \cdot \hat{e}_\beta = g_{\alpha\beta}$ with $\hat{e}_0 = (p_1+p_2)/2$ and $\hat{e}_3 = (p_1-p_2)/2\beta$. In the following we shall often use directly the symbol $J = $ S, V, T, A, P instead of V_J, for example we write V^μ, $T^{\mu\nu}$ instead of V^μ_{V}, $V^{\mu\nu}_{\mathrm{T}}$. The spin projections λ_1 and λ_2 are both taken along the c.m. vector $\vec{e}_3$ i.e. λ_1 and $-\lambda_2$ are the helicities (up to phase conventions). The decomposition is given by

$$S = -2\beta\lambda_-, \quad P = -2|\lambda_-|,$$

$$V^\mu = 2(|\lambda_+|\hat{e}_1^\mu + i\lambda_+\hat{e}_2^\mu - m\lambda_-\hat{e}_3^\mu),$$

$$A^\mu = 2(\beta\lambda_+\hat{e}_1^\mu + i\beta|\lambda_+|\hat{e}_2^\mu - m|\lambda_-|\hat{e}_0^\mu),$$

$$\tfrac{1}{2}T^{\mu\nu} = 2(\lambda_- t_{03}^{\mu\nu} - i\beta|\lambda_-|t_{12}^{\mu\nu} - m|\lambda_+|t_{01}^{\mu\nu} - im\lambda_+ t_{02}^{\mu\nu}), \tag{A.2}$$

where $t^{\mu\nu}_{\alpha\beta} = \hat{e}^\mu_\alpha\hat{e}^\nu_\beta - \hat{e}^\nu_\alpha\hat{e}^\mu_\beta$, $\lambda_\pm = \lambda_1 \pm \lambda_2$. We also use in this paper (for final fermions) other types of vertices

$$\tilde{V}_{J,\lambda_1\lambda_2} = \bar{u}(p_2\lambda_2)\Gamma_J v(p_1\lambda_1). \tag{A.3}$$

They are related to the former ones through simple relations

$$\tilde{V}_{J,\lambda_1\lambda_2} = \pm(V_{J,\lambda_1\lambda_2})^*. \tag{A.4}$$

The minus sign should be used for $J = $ P, T. The vertices $\bar{u}(q_2, \alpha_2)\Gamma_J v(q_1, \alpha_1)$ used in Sections 2 and 3 and in Appendices B and D may be obtained from (A.4) and (A.2) by the formal substitutions $p_i \to q_i$, $\lambda_i \to \alpha_i$, $\hat{e}_a \to \hat{e}'_a$, $\beta \to \beta'$ etc. and by adding in Eq. (A.2) an overall factor $y = ((q_1+q_2)^2/(p_1+p_2)^2)^{1/2}$.

The Fierz identity has the simple form in our notation

$$I_{\alpha\beta}I_{\gamma\delta} = \tfrac{1}{4}\sum_J \Gamma_{J,\alpha\delta}\Gamma^J_{\gamma\beta}. \tag{A.5}$$

Here we introduced the matrices Γ^J which are equal to Γ_J except for two matrices: $\Gamma^{\mathrm{T}} = -\Gamma_{\mathrm{T}}/8$ and $\Gamma^{\mathrm{A}} = -\Gamma_{\mathrm{A}}$. The vertices $V^J = \bar{v}\Gamma^J u$ are related to V_J in the same way.

We now turn to the problem of translating the double spin indices in the density matrix $\varrho_{\alpha_1\bar{\alpha}_1\alpha_2\bar{\alpha}_2}$ into vector indices $a, b = 0, 1, 2, 3$. The relation from Eq. (2.8) may be

rewritten in more formal way as follows:

$$\tilde{A}_+(p, w_a) = \sum_{\alpha\bar{\alpha}} C^+_{a,\alpha\bar{\alpha}} u(p, \alpha)\bar{u}(p, \bar{\alpha}),$$

$$\tilde{A}_-(p, w_a) = \sum_{\alpha\bar{\alpha}} C_{a,\alpha\bar{\alpha}} v(p, \alpha)\bar{v}(p, \bar{\alpha}), \tag{A.6}$$

with $w_i = \hat{e}_i$, $i = 1, 2, 3$ and $w_0 = 0$. The matrices $C^{\pm}$ are simply Clebsch-Gordan coefficients coupling two spins 1/2 into a spin one and spin zero. They have the following form

$$C^{\pm} = \begin{bmatrix} 1 & 1 & 0 & 0 \\ 0 & 0 & \pm 1 & \pm 1 \\ 0 & 0 & -i & i \\ 1 & -1 & 0 & 0 \end{bmatrix}, \tag{A.7}$$

where columns are numbered by $(\alpha\bar{\alpha}) = (++), (--), (+-), (-+)$ and rows by $a = 0, 1, 2, 3$. For the final fermion pair the elements of the density matrix $\varrho_{\alpha_1\bar{\alpha}_1\alpha_2\bar{\alpha}_2}$ come from $v(q_1\alpha_1)\bar{v}(q_1\bar{\alpha}_1) \ldots u(q_2\bar{\alpha}_2)\bar{u}(q_2\alpha_2)$ and they should be translated into vector notation according to[2]

$$U^2 R_{ab} = \sum_{\alpha_i\bar{\alpha}_i} C^-_{a,\alpha_1\bar{\alpha}_1} C^+_{b,\bar{\alpha}_2\alpha_2} \varrho_{\alpha_1\bar{\alpha}_1\alpha_2\bar{\alpha}_2}. \tag{A.8}$$

For example, $\varrho_{\alpha_1\bar{\alpha}_1\alpha_2\bar{\alpha}_2} = \frac{1}{2} U^2 \alpha_+\bar{\alpha}_+$, when substituted into above formula, yields the matrix R with nonzero elements $R_{00} = R_{11} = -R_{22} = R_{33} = 1$. This maping $\alpha_+\bar{\alpha}_+ \Rightarrow \hat{R}_{00} + \hat{R}_{11} - \hat{R}_{22} + \hat{R}_{33}$, together with other relations of this type obtained from Eq. (A.8), read as follows

$$\alpha_+\bar{\alpha}_+ \Rightarrow 2(\hat{R}_{00} + \hat{R}_{11} - \hat{R}_{22} + \hat{R}_{33}),$$

$$|\alpha_+\bar{\alpha}_+| \Rightarrow 2(\hat{R}_{00} - \hat{R}_{11} + \hat{R}_{22} + \hat{R}_{33}),$$

$$\alpha_-\bar{\alpha}_- \Rightarrow 2(\hat{R}_{00} + \hat{R}_{11} + \hat{R}_{22} - \hat{R}_{33}),$$

$$|\alpha_-\bar{\alpha}_-| \Rightarrow 2(\hat{R}_{00} - \hat{R}_{11} - \hat{R}_{22} - \hat{R}_{33}),$$

$$|\alpha_+|\bar{\alpha}_+ + \alpha_+|\bar{\alpha}_+| \Rightarrow 4(\hat{R}_{03} + \hat{R}_{30}), \quad |\alpha_-|\bar{\alpha}_- + \alpha_-|\bar{\alpha}_-| \Rightarrow 4(-\hat{R}_{03} + \hat{R}_{30}),$$

$$|\alpha_+|\bar{\alpha}_+ - \alpha_+|\bar{\alpha}_+| \Rightarrow 4i(\hat{R}_{12} + \hat{R}_{21}), \quad |\alpha_-|\bar{\alpha}_- - \alpha_-|\bar{\alpha}_-| \Rightarrow 4i(-\hat{R}_{12} + \hat{R}_{21}),$$

$$|\alpha_+|\bar{\alpha}_- + \alpha_-|\bar{\alpha}_+| \Rightarrow 4(\hat{R}_{13} + \hat{R}_{31}), \quad |\alpha_-|\bar{\alpha}_+ + \alpha_+|\bar{\alpha}_-| \Rightarrow 4(-\hat{R}_{13} + \hat{R}_{31}),$$

$$|\alpha_+|\bar{\alpha}_- - \alpha_-|\bar{\alpha}_+| \Rightarrow 4i(\hat{R}_{02} + \hat{R}_{20}), \quad |\alpha_-|\bar{\alpha}_+ - \alpha_+|\bar{\alpha}_-| \Rightarrow 4i(-\hat{R}_{02} + \hat{R}_{20}),$$

$$\alpha_+\bar{\alpha}_- + \alpha_-\bar{\alpha}_+ \Rightarrow 4(\hat{R}_{01} + \hat{R}_{10}), \quad |\alpha_+\bar{\alpha}_-| + |\alpha_-\bar{\alpha}_+| \Rightarrow 4(\hat{R}_{01} - \hat{R}_{10}),$$

$$\alpha_+\bar{\alpha}_- - \alpha_-\bar{\alpha}_+ \Rightarrow 4i(\hat{R}_{23} + \hat{R}_{32}), \quad |\alpha_+\bar{\alpha}_-| - |\alpha_-\bar{\alpha}_+| \Rightarrow 4i(-\hat{R}_{23} + \hat{R}_{32}). \tag{A.9}$$

[2] In the case of the hard bremsstrahlung factor U^2 in Eq. (A.8) should be replaced by e^2U^2.

This is the complete set of relations for one fermion-antifermion pair which translate the double spin index into a vector index.

In the last part of this Appendix we shall show how one should connect the density matrix of the produced unstable spin 1/2 fermion with the decay differential cross section.

In spinor notation, let us denote the production amplitude as $\bar{u}(q)M_1$ and the decay amplitude as $\bar{M}_2 u(q)$. They are combined with the fermion propagator as follows:

$$M_c \sim \bar{M}_2(\not{q}+M)M_1. \tag{A.10}$$

The differential cross section for production and decay is

$$|M_c|^2 \sim \bar{M}_2 \frac{\not{q}+M}{2M} M_1 \bar{M}_1 \frac{\not{q}+M}{2M} M_2 = X. \tag{A.11}$$

Using twice the Fierz identity it may be rewritten as

$$X = \tfrac{1}{16} \sum_{I,J} \bar{M}_1 L \Gamma_I L M_1 \operatorname{Tr}(\Gamma^I L \Gamma^J L) \bar{M}_2 L \Gamma_J L M_2, \tag{A.12}$$

where $L = L^2 = (\not{q}+M)/2M$. All traces can easily be calculated and using $\not{q}L = L\not{q} = M\not{q}$ we obtain

$$X = \tfrac{1}{2}\left[\bar{M}_1 L M_1 \bar{M}_2 L M_2 - \bar{M}_1 L \gamma_5 \gamma^\mu M_1 \left(g_{\mu\nu} - \frac{q_\mu q_\nu}{M^2}\right) \bar{M}_2 L \gamma_5 \gamma^\nu M_2\right]$$

$$= \tfrac{1}{2}(R_0 h_0 + \sum_{i=1}^{3} R_i h_i), \tag{A.13}$$

where

$$\bar{M}_1 L(1+\gamma_5 \not{w}) M_1 = R_0 + \sum_{i=1}^{3} R_i w^i,$$

$$\bar{M}_2 L(1+\gamma_5 \not{w}) M_2 = h_0 + \sum_{i=1}^{3} h_i w^i$$

$$w \cdot q = 0, \qquad w = (0, \vec{w}).$$

The tau rest system, $q = (M, 0, 0, 0)$, was used in the last two equations.

The decomposition (A.13) generalizes easily to two or more fermions. Eq. (5.4) is a direct generalization of (A.13) to the case of a fermion-antifermion pair.

APPENDIX B

The contribution from one uncrossed box diagram may be written as follows:

$$M^a_{\lambda_i \alpha_i} = (e^2 Q Q')^2 (2\pi)^{-4} \int_k \bar{v}(p_1\lambda_1)\gamma^\mu \not{k}_1 \gamma^\nu u(p_2\lambda_2)\bar{u}(q_2\alpha_2)\gamma_\nu(\not{k}_2+M)\gamma_\mu v(q_1\alpha_1), \tag{B.1}$$

where

$$k_1 = k-\beta q, \quad k_2 = k-\beta' q',$$

$$\int_k f(k) = \int \frac{d^4k f(k)}{F_1 F_2 F_+ F_-},$$

$$F_1 = k^2-2\beta k\cdot q-1+i\varepsilon, \quad F_2 = k^2-2\beta' k\cdot q'-1+i\varepsilon$$

$$F_\pm = k^2 \pm 2k\cdot\pi+1+i\varepsilon, \quad \pi = (p_1+p_2)/2, \quad q = (p_1-p_2)/2\beta.$$

The vector q' is defined in Section 2. The electron mass will be neglected in the numerator of the integral.

Using twice the Fierz identity, see Eq. (A.5), we separate the initial and final pairs of spinors in the form of the Fierz vertices V_I and $\tilde{V}_{\tilde{J}}$ which were given in Appendix A

$$M^{\mathrm{a}}_{\lambda_i\alpha_i} = (e^2QQ')^2(2\pi)^{-4}\int_k \tfrac{1}{16}\sum_{I,\tilde{J}} \bar{v}(p_1\lambda_1)\Gamma^I u(p_2\lambda_2)$$

$$\times \mathrm{Tr}\,(\Gamma_I\gamma^\mu \not{k}_1\gamma^\nu)\,\mathrm{Tr}\,(\gamma_\nu(\not{k}_2+M)\gamma_\mu\Gamma^{\tilde{J}})\bar{u}(q_2\alpha_2)\Gamma^{\tilde{J}}v(q_1\alpha_1)$$

$$= (e^2QQ')^2(2\pi)^{-4}\int_k \sum_{I\tilde{J}} V^I S_{I\tilde{J}}\tilde{V}^{\tilde{J}}. \tag{B.2}$$

Out of the 25 elements of $S_{I\tilde{J}}$, only five are non-zero which can be calculated easily:

$$M_{\mathrm{V}\tilde{\mathrm{V}}} = V_\mu S^{\mu\nu}_{\mathrm{V}\tilde{\mathrm{V}}}\tilde{V}_\nu = 2V\cdot\tilde{V}k_1\cdot k_2+2\tilde{V}\cdot k_1 V\cdot k_2,$$

$$M_{\mathrm{A}\tilde{\mathrm{A}}} = A_\mu S^{\mu\nu}_{\mathrm{A}\tilde{\mathrm{A}}}A_\nu = -2A\cdot\tilde{A}k_1\cdot k_2+2\tilde{A}\cdot k_1 A\cdot k_2,$$

$$M_{\mathrm{V}\tilde{\mathrm{S}}} = V_\mu S^\mu_{\mathrm{V}\tilde{\mathrm{S}}}\tilde{S} = -2MV\cdot k_1\tilde{S},$$

$$M_{\mathrm{A}\tilde{\mathrm{T}}} = A_\mu S^{\mu\nu\lambda}_{\mathrm{A}\tilde{\mathrm{T}}}\tfrac{1}{2}\tilde{T}_{\lambda\nu} = \tfrac{1}{2}iM\varepsilon_{\alpha\mu\nu\lambda}k_1^\alpha A^\mu\tilde{T}^{\nu\lambda}. \tag{B.3}$$

As it was shown in Appendix A, all Fierz vertices can be expressed in terms of basic vectors $\{\hat{e}_a\} = (\pi, \tau, \sigma, q)$ and $\{e'_a\} = (\pi, \tau, \sigma', q')$, $a = 0, 1, 2, 3$, where $\tau, \sigma, \sigma', q'$ were defined in Section 2

$$V = 2(|\lambda_+|\tau+i\lambda_+),$$

$$A = 2(\lambda_+\tau+i|\lambda_+|\sigma),$$

$$\tilde{V} = 2(|\alpha_+|\tau-i\alpha_+\sigma'-M\alpha_- q'),$$

$$\tilde{A} = 2(\alpha_+\beta'\tau-i|\alpha_+|\beta'\sigma'-M|\alpha_-|\pi),$$

$$\tfrac{1}{2}\tilde{T} = 2(-\alpha_-[\pi, q']-i|\alpha_-|\beta'[\tau, \sigma']+|\alpha_+|M[\pi, \tau]-i\alpha_+ M[\pi, \sigma'],$$

$$\tilde{S} = -2\beta'\alpha_-,$$

$$[a, b]^{\mu\nu} = a^\mu b^\nu - a^\nu b^\mu. \tag{B.4}$$

We now substitute Eqs. (B.4) into $M^a = M_{V\tilde{V}} + M_{A\tilde{A}} + M_{V\tilde{S}} + M_{A\tilde{T}}$, obtaining as a result Eq. (3.4) with the following expressions for functions X_i:

$$X_0 = 2(1-\beta' c)\frac{4}{\pi^2}\int_k 1,$$

$$X_1 = \frac{4}{\pi^2}\int_k [-(k\cdot\tau)^2 - \beta'(k\cdot\sigma)(k\cdot\sigma') - (1-\beta' c)(1-k^2)],$$

$$X_2 = \frac{4}{\pi^2}\int_k [-\beta'(k\cdot\tau)^2 - (k\cdot\sigma)(k\cdot\sigma') + 2(\beta'-c)k\cdot\varrho$$

$$+2(1-\beta' c)k\cdot\varrho' + (\beta'-c)(1-k^2)],$$

$$sX_3 = \frac{4}{\pi^2}\int_k [-(k\cdot\varrho')^2 + c(k\cdot\varrho)(k\cdot\varrho') + c(2c-\beta')k\cdot\varrho$$

$$+(2\beta' c^2 - 2c - \beta')k\cdot\varrho' - s^2(1-k^2)]. \tag{B.5}$$

All integrals of the type $\int_k k\cdot\varrho$, $\int_k (k\cdot\varrho)(k\cdot\varrho')$, $\int_k k^2$ etc. may be expressed in terms of seven functions B_j given by the following formulae:

$$B_1 = \frac{4}{\pi^2}\int_k 1 = iA\ln\frac{\lambda^2}{4} - \pi A,$$

$$B_2 = iA,$$

$$B_3 = \frac{2}{\pi^2}\int_k (1-k^2) = iB - \pi A,$$

$$B_4 = F'_\Delta = 4F_\Delta/\pi^2,$$

$$B_5 = F'_\varrho = 4F_\varrho/\pi^2,$$

$$B_6 = i\ln\frac{4}{m^2} + \pi,$$

$$B_7 = i\ln\frac{4}{M^2} + \pi. \tag{B.6}$$

The real functions A and B and the complex function F_ϱ and F_Δ are defined in Ref. [2]. In order to obtain the final result for the function X_i we first eliminate $(k\cdot\tau)^2$ using the identity $k^2 = (k\cdot\pi)^2 - (k\cdot\tau)^2 - (k\cdot\sigma)^2 - (k\cdot\varrho)^2$, then we express σ and σ' in terms

TABLE V

The coefficients d_{ik} in the decomposition of the typical box integrals $\frac{4}{\pi^2}\int_k f_i(k) = \sum_{j=1}^{7} d_{ij}B_j$. The functions B_j are defined in Eq. (B.6)

f_i \ j	1	2	3	4	5	6	7
$k\cdot\varrho$	0	0	-1	0	$-\frac{1}{2}$	0	0
$\beta' k\cdot\varrho'$	0	0	-1	$-\frac{1}{2}$	0	0	0
$(k\cdot\pi)^2$	1	2	-1	0	0	0	0
$(k\cdot\varrho)^2$	0	$\frac{2\beta'^2 s^2}{\omega}$	1	0	$\frac{1}{2}\left(1+\frac{c}{\beta'}\right)$	$\frac{1-\beta' c}{\omega}$	$-\frac{1-\beta' c}{\omega}-\frac{c}{\beta'}$
$\beta'^2(k\cdot\varrho')^2$	0	$\frac{2\beta'^2 s^2}{\omega}$	1	$\frac{1}{2}(1+\beta' c)$	0	$-\frac{\beta'(\beta'-c)}{\omega}-\beta' c$	$\frac{\beta'(\beta'-c)}{\omega}$
$\beta'(k\cdot\varrho)(k\cdot\varrho')$	0	$\frac{2\beta'^2 s^2}{\omega}$	1	$\frac{1}{2}$	$\frac{1}{2}$	$-\frac{\beta'(\beta'-c)}{\omega}$	$-\frac{1-\beta' c}{\omega}$

of ϱ and ϱ' and finally all k-integrals in X_i may be found in Table V. In formula (3.5) we introduced for convenience the functions $\tilde{A} = 2(1-\beta' c)A$ and $\tilde{B} = 2(1-\beta' c)B$. In Ref. [1] the four functions $\tilde{A}$, $\tilde{B}$, $\mathrm{Im}\,F'_A$ and $\mathrm{Im}\,F'_Q$ were calculated in the limit $m \to 0$. We list them for the sake of completeness including also real parts of F'_A and F'_Q

$$\tilde{A} = 2\ln\frac{1-\beta' c}{2} + \ln\frac{4}{m^2} + \ln\frac{4}{M^2},$$

$$\tilde{B} = \ln^2\frac{1-\beta' c}{2} - 2\,\mathrm{Li}_2\frac{2-2\beta' c-M^2}{2(1-\beta' c)} - \tfrac{1}{2}\ln^2\frac{4}{m^2} - \tfrac{1}{2}\ln^2\frac{4}{M^2},$$

$$F'_A = i\left(\tfrac{1}{2}\ln^2\frac{4}{m^2} + \frac{\pi^2}{6}\right) + \pi\ln\frac{4}{m^2},$$

$$F'_Q = \frac{i}{\beta'}\left(\tfrac{1}{2}\ln^2\frac{1+\beta'}{1-\beta'} + 2\,\mathrm{Li}_2\left(\frac{-1+\beta'}{1+\beta'}\right) + \frac{\pi^2}{6}\right) + \frac{\pi}{\beta'}\ln\frac{1+\beta'}{1-\beta'}. \qquad \text{(B.7)}$$

APPENDIX C

In this Appendix we present the formulae for the hard bremsstrahlung differential cross section $A(w_1, w_2)$ in Eq. (4.2) obtained using standard methods, i.e. projection operators defined in Eq. (2.4) and an algebraic computer program [10]. We give separately the results for initial and final state radiation and for their interference:

$$A(w_1, w_2) = A_{\mathrm{ini}}(w_1, w_2) + A_{\mathrm{fin}}(w_1, w_2) + A_{\mathrm{int}}(w_1, w_2), \qquad \text{(C.1)}$$

with

$$A_{\text{ini}}(w_1, w_2) = (1 - w_1 \cdot w_2) A_{\text{ini}}$$

$$+ \frac{Q^2}{x_1 x_2 \tilde{s}_1} \left\{ w_1 \cdot w_2 \left((\tilde{t} + \tilde{u})^2 + (\tilde{t}_1 + \tilde{u}_1)^2 - m^2 \tilde{s}_1 \left(\frac{x_1}{x_2} + \frac{x_2}{x_1} \right) \right) \right.$$

$$- 2a_1 b_1 x_2 - 2a_2 b_2 x_1 + 2((a_3 b_1 - a_2 b_1)\tilde{t} + (a_1 b_3 - a_1 b_2)\tilde{u}) \left(1 - \frac{m^2}{\tilde{s}_1} \frac{x_1}{x_2} \right)$$

$$\left. + 2((a_2 b_3 - a_2 b_1)\tilde{t}_1 + (a_3 b_2 - a_1 b_2)\tilde{u}_1) \left(1 - \frac{m^2}{\tilde{s}_1} \frac{x_2}{x_1} \right) \right\},$$

$$A_{\text{fin}}(w_1, w_2) = (1 - w_1 \cdot w_2) A_{\text{fin}}$$

$$+ \frac{Q'^2}{y_1 y_2 \tilde{s}} \left\{ w_1 \cdot w_2 \left(x_1^2 + x_2^2 + 2\tilde{s}\tilde{s}_1 - M^2 \tilde{s} \left(2 + \frac{y_1}{y_2} + \frac{y_2}{y_1} \right) \right) \right.$$

$$- (a_1 b_2 + a_2 b_1) \left(\tilde{s} + \tilde{s}_1 - M^2 \left(2 + \frac{y_1}{y_2} + \frac{y_2}{y_1} \right) \right)$$

$$+ (a_1 b_2 - a_2 b_1) \left((\tilde{t} - \tilde{u}_1) \left(1 - \frac{M^2}{\tilde{s}} \left(1 + \frac{y_1}{y_2} \right) \right) + (\tilde{t}_1 - \tilde{u}) \left(1 - \frac{M^2}{\tilde{s}} \left(1 + \frac{y_2}{y_1} \right) \right) \right)$$

$$- 2a_1 b_1 x_2 - 2a_2 b_2 x_1 + a_1 b_3 \left(2\tilde{u} - M^2 \left(1 + \frac{y_1}{y_2} \right) \right) + a_2 b_3 \left(2\tilde{t}_1 - M^2 \left(1 + \frac{y_1}{y_2} \right) \right)$$

$$\left. + a_3 b_1 \left(2\tilde{t} - M^2 \left(1 + \frac{y_2}{y_1} \right) \right) + a_3 b_2 \left(2\tilde{u}_1 - M^2 \left(1 + \frac{y_2}{y_1} \right) \right) \right\},$$

$$A_{\text{int}}(w_1, w_2) = (1 - w_1 \cdot w_2) A_{\text{int}}$$

$$+ \frac{QQ'}{\tilde{s}\tilde{s}_1 x_1 x_2 y_1 y_2} \{ (\tilde{t} x_2 y_2 + \tilde{t}_1 x_1 y_1 - \tilde{u} x_2 y_1 - \tilde{u}_1 x_1 y_2) (w_1 \cdot w_2 (\tilde{t} + \tilde{u})^2$$

$$+ w_1 \cdot w_2 (\tilde{t}_1 + \tilde{u}_1)^2 - 2a_1 b_1 x_2 - 2a_2 b_2 x_1 + 2a_1 b_3 u + 2a_3 b_2 \tilde{u}_1 + 2a_3 b_1 \tilde{t}$$

$$+ 2a_2 b_3 \tilde{t}_1 - 2a_2 b_1 (\tilde{t} + \tilde{t}_1) - 2a_1 b_2 (\tilde{u} + \tilde{u}_1))$$

$$- M^2 (\tilde{s} - \tilde{s}_1) ((a_1 b_3 - a_3 b_1)\tilde{s} x_2 + (a_3 b_2 - a_2 b_3)\tilde{s} x_1 + 2(a_2 b_1 - a_1 b_2) x_1 x_2) \}, \qquad \text{(C.2)}$$

where

$$\tilde{s} = p_1 \cdot p_2, \quad \tilde{t} = p_1 \cdot q_1, \quad \tilde{u} = p_1 \cdot q_2,$$

$$\tilde{s}_1 = q_1 \cdot q_2, \quad \tilde{t}_1 = p_2 \cdot q_2, \quad \tilde{u}_1 = p_2 \cdot q_1,$$

$$a_1 = w_1 \cdot p_1, \quad a_2 = w_1 \cdot p_2, \quad a_3 = w_1 \cdot k,$$

$$b_1 = w_2 \cdot p_1, \quad b_2 = w_2 \cdot p_2, \quad b_3 = w_2 \cdot k.$$

We used the same definitions for A_{ini}, A_{fin} and A_{int} as in Ref. [1].

APPENDIX D

In this Appendix we shall calculate one of the two bremsstrahlung factors $\tilde{H}^{\mu}_{\alpha_i\gamma}$. The derivation of $H^{\mu}_{\lambda_i\gamma}$ is completely analogous. As in the case of the box diagrams, we isolate the final state spinors in Eq. (4.10) using the Fierz identity for each one of the two terms in Eq. (4.10). For example, the first term may be rewritten as

$$\frac{1}{8k\cdot q_1}\sum_{\tilde{\jmath}}\operatorname{Tr}(\gamma^{\mu}(-\not{q}_1-\not{k}+M)\varepsilon_{\gamma}\Gamma^{\tilde{\jmath}})\bar{u}(q_2\alpha_2)\Gamma_{\tilde{\jmath}}v(q_1\alpha_1). \tag{D.1}$$

Some of the traces vanish and $\tilde{H}$ takes the following form

$$\begin{aligned}\tilde{H}^{\mu}_{\alpha_i\gamma} = {} & \frac{1}{2k\cdot q_1}\{-\tfrac{1}{4}\operatorname{Tr}(\gamma^{\mu}(\not{k}+\not{q}_1)\not{\varepsilon}_{\gamma}\gamma^{\nu})\tilde{V}_{\nu}\\ & +\tfrac{1}{4}\operatorname{Tr}(\gamma^{\mu}(\not{k}+\not{q}_1)\not{\varepsilon}_{\gamma}\gamma_5\gamma^{\nu})\tilde{A}_{\nu}+M\tilde{S}\varepsilon^{\mu}_{\gamma}+\tfrac{1}{2}M\tilde{T}^{\mu\nu}(\varepsilon_{\gamma})_{\nu}\}\\ & +\frac{1}{2k\cdot q_2}\{\tfrac{1}{4}\operatorname{Tr}(\gamma^{\mu}(\not{k}+\not{q}_2)\not{\varepsilon}_{\gamma}\gamma^{\nu})\tilde{V}_{\nu}+\tfrac{1}{4}\operatorname{Tr}(\gamma^{\mu}(\not{k}+\not{q}_2)\not{\varepsilon}_{\gamma}\gamma_5\gamma^{\nu})\tilde{A}_{\nu}\\ & +M\tilde{S}\varepsilon^{\mu}_{\gamma}-\tfrac{1}{2}M\tilde{T}^{\mu\nu}(\varepsilon_{\gamma})_{\nu}\}.\end{aligned} \tag{D.2}$$

We substitute in this equation the Fierz vertices, which are taken from Appendix A:

$$\begin{aligned}\tilde{S} &= -2yv\alpha_-, \qquad \tilde{P} = 2y|\alpha_-|,\\ \tilde{V} &= 2y(|\alpha_+|\hat{e}'_1-i\alpha_+\sigma'-\tilde{M}\alpha_-\varrho'),\\ \tilde{A} &= 2y(\alpha_+v\hat{e}'_1-i|\alpha_+|v\sigma'-\tilde{M}|\alpha_-|\hat{e}'_0),\\ \tfrac{1}{2}\tilde{T}_{\mu\nu} &= 2y(-\alpha_-[\hat{e}'_0,\varrho']-i|\alpha_-|v[\hat{e}'_1,\sigma']\\ &\quad +|\alpha_+|\tilde{M}[\hat{e}'_0,\hat{e}'_1]-i\alpha_+\tilde{M}[\hat{e}'_0,\sigma'],\end{aligned}$$

where $\sigma' = c_2\hat{e}'_2-s_2\hat{e}'_3$, $\varrho' = s_2\hat{e}'_2+c_2\hat{e}'_3$. As a result we obtain $\tilde{H}$ as given in Eq. (4.11). The function $H^{\mu}_{\lambda_i\gamma}$ may be obtained from $\tilde{H}^{\mu}_{\alpha_i\gamma}$ by formal substitutions $\alpha_i \to \lambda_i$, $c_1 \to c_2$, $s_1 \to -s_2$, $\tilde{M} \to m$, $k \to -\bar{k}$, $\hat{e}'_i \to \hat{e}_i$, or by direct calculation in the same way as $\tilde{H}$.

REFERENCES

[1] F. A. Berends, R. Kleiss, S. Jadach, Z. Wąs, *Acta Phys. Pol.* **B14**, 413 (1983).

[2] F. A. Berends, K. J. F. Gaemers, R. Gastmans, *Nucl. Phys.* **B63**, 381 (1973) and *Nucl. Phys.* **B57**, 381 (1973).

[3] F. A. Berends, R. Kleiss, *Nucl. Phys.* **B177**, 237 (1981).

[4] F. A. Berends, R. Kleiss, P. De Causmaecker, R. Gastmans, T. T. Wu, *Phys. Lett.* **103B**, 124 (1981).

[5] F. A. Berends, R. Kleiss, S. Jadach, *Nucl. Phys.* **B202**, 63 (1982).

[6] F. A. Berends, R. Kleiss, S. Jadach, *Comp. Phys. Commun.* **29**, 185 (1983).
[7] Young-Su Tsai, *Phys. Rev.* **D4**, 2821 (1971).
[8] H. J. Behrend et al., τ Branching ratios and polarisation limits..., Preprint DESY 83-019, to be published in *Phys. Lett.*
[9] S. Jadach, Z. Wąs, Monte Carlo simulation of the process $e^+e^- \to \tau^+\tau^-$, $\tau^\pm \to X^\pm$ including radiative $O(\alpha^3)$ QED corrections, mass and spin effects. *Comp. Phys. Commun.*, in print.
[10] M. Veltman, SCHOONSHIP a CDC algebraic program, CERN preprint (1967), H. Strubbe, *Comp. Phys. Commun.* **8**, 1 (1974).
[11] S. Glashow, *Nucl. Phys.* **22**, 579 (1961); S. Wainberg, *Phys. Rev. Lett.* **19**, 1264 (1967); A. Salam, in *Elementary Particle Theory*, ed. M. Svartholm, Stockholm 1968.